Phenomenology of Higgs bosons in the Zee-Model

Shinya Kanemura[1,2*], Takashi Kasai[3,4†], Guey-Lin Lin[5‡],

Yasuhiro Okada[3,6§], Jie-Jun Tseng[5**], and C.-P. Yuan[2,7††]

[1] Institut für Theoretische Physik, Universität Karlsruhe, D-76128 Karlsruhe, Germany

[2] Physics and Astronomy Department, Michigan State University, East Lansing, MI 48824-1116, USA

[3] Theory Group, KEK, Tsukuba, Ibaraki, 305-0801 Japan

[4] Department of Accelerator Science, The Graduate University for Advanced Studies, Tsukuba, Ibaraki, 305-0801 Japan

[5] National Chiao Tung University, Hsinchu 300, Taiwan

[6] Department of Particle and Nuclear Physics, The Graduate University for Advanced Studies, Tsukuba, Ibaraki, 305-0801 Japan

[7] Theory Division, CERN, CH-1211, Geneva, Switzerland

To appear in Physical Review D

*Email: kanemu@particle.physik.uni-karlsruhe.de

†Email: kasai@post.kek.jp

‡Email: glin@cc.nctu.edu.tw

§Email: yasuhiro.okada@kek.jp

**Email: u8627512@cc.nctu.edu.tw

††Email: yuan@pa.msu.edu

Abstract

To generate small neutrino masses radiatively, the Zee-model introduces two Higgs doublets and one weak-singlet charged Higgs boson to its Higgs sector. From analyzing the renormalization group equations, we determine the possible range of the lightest CP-even Higgs boson (h) mass and the Higgs boson self-couplings as a function of the cut-off scale beyond which either some of the coupling constants are strong enough to invalidate the perturbative analysis or the stability of the electroweak vacuum is no longer guaranteed. Using the results obtained from the above analysis, we find that the singlet charged Higgs boson can significantly modify the partial decay width of $h \to \gamma\gamma$ via radiative corrections, and its collider phenomenology can also be drastically different from that of the charged Higgs bosons in the usual two-Higgs-doublet models.

PACS number(s): 13.15. +g, 14.80.Cp.

hep-ph/0011357, KA-TP-18-2000, KEK-TH-706, NCTU-HEP-0004, CERN-TH/2000-228

I. INTRODUCTION

From the atmospheric and solar neutrino data, there is increasing evidence for neutrino oscillations [1]. If this is a correct interpretation, the Standard Model (SM) has to be extended to incorporate the small masses of the neutrinos suggested by data. There have been several ideas proposed in literature to generate small neutrino masses. The Zee-model is one of such attempts [2–6]. In this model, all flavor neutrinos are massless at the tree level, and their small masses are induced radiatively through one-loop diagrams. For such a mass-generation mechanism to work, it is necessary to extend the Higgs sector of the SM to contain at least two weak-doublet fields and one weak-singlet charged scalar field. Although some studies have been done to examine the interaction of the leptons and the Higgs bosons in the Zee-model [7], the scalar (Higgs) sector of the model remains unexplored in detail. In this paper we study the Higgs sector of the Zee-model to clarify its impact on the Higgs search experiments, either at the CERN LEP-II, the Run-II of the Fermilab Tevatron, the CERN Large Hadron Collider (LHC), or future linear colliders (LC's).

Experimental search for the Higgs boson has been continued at the CERN LEP and the Fermilab Tevatron experiments. In the LEP-II experiments, the Higgs boson with the mass less than about 110 GeV has been excluded if its production cross section and decay modes are similar to those of the SM Higgs boson [8]. Run-II of the Tevatron can be sensitive to a SM-like Higgs boson with the mass up to about 180 GeV, provided that the integrated luminosity of the collider is large enough (about $30\,\mathrm{fb}^{-1}$) [9]. Furthermore, the primary goal of the CERN LHC experiments is to guarantee the discovery of a SM-like Higgs boson for its mass as large as about 1 TeV [10], which is the upper bound of the SM Higgs boson mass. (For a Higgs boson mass beyond this value, the SM is no longer a consistent low energy theory.)

When the Higgs boson is discovered, its mass and various decay properties will be measured to test the SM and to distinguish models of new physics at high energy scales. For example, the allowed mass range of the lightest CP-even Higgs boson (h) can be determined

by demanding the considered theory to be a valid effective theory all the way up to some cut-off energy scale (Λ). For $\Lambda = 10^{19}$ GeV (i.e., the Planck scale), the lower and upper bounds of the SM Higgs boson masses are 137 GeV and 175 GeV, respectively [11]. The Higgs mass bounds for the two-Higgs-doublet-model (THDM) were also investigated [12,13] with and without including the soft-breaking term with respect to the discrete symmetry that protects the natural flavor conservation. It was found in Ref. [13] that the lower bound of the lightest CP-even Higgs boson is about 100 GeV in the decoupling regime where only one neutral Higgs boson is light as compared to the other physical states of Higgs bosons.

The Higgs sector of the Zee-model is similar to that of the THDM except for the existence of an additional weak-singlet charged Higgs field, so that the physical scalar bosons include two CP-even, one CP-odd and two pairs of charged Higgs bosons. In this paper, we shall first determine the upper and lower bounds for the lightest CP-even Higgs boson mass (m_h) as a function of the cut-off scale Λ of the Zee-model, using renormalization group equations (RGE's).[1] We show that the upper and lower mass bounds for h are almost the same as those in the THDM. We also study the possible range of the Higgs-boson self-coupling constants at the electroweak scale as a function of Λ. By using these results, we examine effects of the additional loop contribution of the singlet charged Higgs boson to the partial decay width of $h \to \gamma\gamma$. We show that, by taking $\Lambda = 10^{19}$ GeV, the deviation of the decay width from the SM prediction can be about -20% or nearly $+10\%$ for m_h between 125 GeV and 140 GeV when the mass of the isospin singlet charged Higgs boson is taken to be around 100 GeV. The magnitude of the deviation becomes larger for lower cutoff scales and smaller masses of the singlet charged Higgs boson. If we choose $\Lambda = 10^4$ GeV and the singlet charged Higgs boson mass to be 100 GeV, the positive deviation can be greater than $+30\%$ ($+40\%$) for $m_h = 125$ GeV (140 GeV). Such a deviation from the SM prediction could be tested at the

[1]For the model with see-saw mechanism for neutrino mass generation the Higgs mass bound has been studied as a function of cut-off scale in Ref. [14].

LHC, the e^+e^- LC and the $\gamma\gamma$ option of LC [15–17]. We also discuss phenomenology of the singlet charged Higgs boson at present and future collider experiments, which is found to be completely different from that of the ordinary THDM-like charged Higgs bosons. To detect such a charged Higgs boson at LEP-II experiments, experimentalists have to search for their data sample with $e^\pm$ or $\mu^\pm$ plus missing energy, in contrast to the usual detection channels: either $\tau\nu$ or cs decay modes.

This paper is organized as follows. In Sec. II, we introduce the Higgs sector of the Zee-model and review the neutrino masses and mixings in this model which are consistent with the atmospheric and solar neutrino observations. Numerical results on the possible range of the mass and coupling constants of the Higgs bosons are given in Sec. III. In Sec IV, we discuss the one-loop effect of the extra-Higgs bosons in the Zee-model to the partial decay width of $h \to \gamma\gamma$ and its impacts on the neutral Higgs-boson search at high-energy colliders. The phenomenology of the charged Higgs boson that comes from the additional singlet field is discussed in Sec. V. In Sec. VI, we present additional discussions and conclusion. Relevant RGE's for the Zee-model are given in the Appendix.

II. ZEE-MODEL

To generate small neutrino mass radiatively, the Zee-model contains a $SU(2)_L$ singlet charged scalar field ω^-, in addition to two $SU(2)_L$ doublet fields ϕ_1, and ϕ_2. The Zee-model Lagrangian is written as:

$$\mathcal{L} = \mathcal{L}_{kin} + \mathcal{L}_{ll\omega} + \mathcal{L}_{Yukawa} - V(\phi_1, \phi_2, \omega^-)\,, \tag{1}$$

where

$$\begin{aligned}\mathcal{L}_{kin} = &|D_\mu\phi_1|^2 + |D_\mu\phi_2|^2 + \left|D_\mu\omega^-\right|^2 + i\overline{q_{_L}}\gamma^\mu D_\mu q_{_L} + i\overline{u_{_R}}\gamma^\mu D_\mu u_{_R} + i\overline{d_{_R}}\gamma^\mu D_\mu d_{_R} \\ &+ i\overline{l_{_L}}\gamma^\mu D_\mu l_{_L} + i\overline{e_{_R}}\gamma^\mu D_\mu e_{_R} + \sum_{a=SU(3),SU(2),U(1)} \frac{1}{4}F_{\mu\nu}^{a^2}\,,\end{aligned} \tag{2}$$

$$\mathcal{L}_{ll\omega} = f_{ij}\overline{l_{i_L}}(i\tau_2)(l_{j_L})^C\omega^- + f_{ij}\overline{l_{i_L}}^C(i\tau_2)l_{j_L}\omega^+, \tag{3}$$

where i, j $(= 1, 2, 3)$ are the generation indices, and

$$\begin{aligned} V(\phi_1, \phi_2, \omega^-) = & \, m_1^2 \left|\phi_1\right|^2 + m_2^2 \left|\phi_2\right|^2 + m_0^2 \left|\omega^-\right|^2 \\ & - m_3^2 (\phi_1^\dagger \phi_2 + \phi_2^\dagger \phi_1) - \mu \widetilde{\phi_1}^T i\tau_2 \widetilde{\phi_2}\, \omega^- + \mu \phi_2^T i\tau_2 \phi_1\, \omega^+ \\ & + \frac{1}{2}\lambda_1 \left|\phi_1\right|^4 + \frac{1}{2}\lambda_2 \left|\phi_2\right|^4 + \lambda_3 \left|\phi_1\right|^2 \left|\phi_2\right|^2 \\ & + \lambda_4 \left|\phi_1^\dagger \phi_2\right|^2 + \frac{\lambda_5}{2}\left[\left(\phi_1^\dagger \phi_2\right)^2 + \left(\phi_2^\dagger \phi_1\right)^2\right] \\ & + \sigma_1 \left|\omega^-\right|^2 \left|\phi_1\right|^2 + \sigma_2 \left|\omega^-\right|^2 \left|\phi_2\right|^2 + \frac{1}{4}\sigma_3 \left|\omega^-\right|^4 . \end{aligned} \tag{4}$$

In the above equations, q_L is the left-handed quark doublet with an implicit generation index while u_R and d_R denote the right-handed singlet quarks. Similarly, l_L and e_R denote the left-handed and right-handed leptons in three generations. The charge conjugation of a fermion field is defined as $\psi^C \equiv C\overline{\psi}^T$, where C is the charge conjugation matrix ($C^{-1}\gamma^\mu C = -\gamma^{\mu T}$) with the super index T indicating the transpose of a matrix. Also, $\phi_m = \begin{pmatrix} \phi_m^0 \\ \phi_m^- \end{pmatrix}$ and $\widetilde{\phi_m} \equiv (i\tau_2)\, \phi_m^*$ with $m = 1, 2$. Without loss of generality, we have taken the anti-symmetric matrix f_{ij} and the coupling μ to be real in the equations (3) and (4). In order to suppress flavor changing neutral current (FCNC) at the tree level, a discrete symmetry, with $\phi_1 \to \phi_1$, $\phi_2 \to -\phi_2$, $\omega^+ \to +\omega^+$, is imposed to the Higgs sector of the Lagrangian, which is only broken softly by the m_3^2 term and the μ term. Under the discrete symmetry there are two possible Yukawa-interactions; that is, for type-I

$$\mathcal{L}_{Yukawa-I} = \overline{d_{_{R_i}}} \left(y_{_D} V_{CKM}^\dagger\right)_{ij} \widetilde{\phi_2}^\dagger q_{_{L_j}} + \overline{u_{_{R_i}}} \left(y_{_U}\right)_{ii} \phi_2^\dagger q_{_{L_i}} + \overline{e_{_{R_i}}} \left(y_{_E}\right)_{ii} \widetilde{\phi_2}^\dagger l_{_{L_i}} + h.c.\,, \tag{5}$$

and for type-II,

$$\mathcal{L}_{Yukawa-II} = \overline{d_{_{R_i}}} \left(y_{_D} V_{CKM}^\dagger\right)_{ij} \widetilde{\phi_1}^\dagger q_{_{L_j}} + \overline{u_{_{R_i}}} \left(y_{_U}\right)_{ii} \phi_2^\dagger q_{_{L_i}} + \overline{e_{_{R_i}}} \left(y_{_E}\right)_{ii} \widetilde{\phi_1}^\dagger l_{_{L_i}} + h.c.\,, \tag{6}$$

where $y_{_U}$,$y_{_D}$,$y_{_E}$ are diagonal Yukawa matrices and V_{CKM} is the Cabibbo-Kobayashi-Maskawa (CKM) matrix. Later, we shall only keep the top Yukawa coupling constants $y_t = \left(y_{_U}\right)_{33}$

in our numerical evaluation of the RGE's[2]. In that case, there is no difference between the Yukawa couplings of the type-I and the type-II models. Finally, for simplicity, we assume that all λ_i and m_i^2 are real parameters.

Let us now discuss the Higgs sector. The $SU(2)_L \times U(1)_Y$ symmetry is broken to $U(1)_{em}$ by $\langle\phi_1\rangle$ and $\langle\phi_2\rangle$, the vacuum expectation values of ϕ_1 and ϕ_2. (They are assumed to be real so that there is no spontaneous CP violation.) The number of physical Higgs bosons are two CP-even Higgs bosons (H,h), one CP-odd Higgs boson (A) and two pairs of charged Higgs boson ($S_1^\pm$, $S_2^\pm$). We take a convention of $m_H > m_h$ and $m_{S_1} > m_{S_2}$. In the basis where two Higgs doublets are rotated by the angle β, with $\tan\beta = \frac{\langle\phi_2^0\rangle}{\langle\phi_1^0\rangle}$, the mass matrices for the physical states of Higgs bosons are given by

$$M_N^2 = \begin{bmatrix} \left(\lambda_1 \cos^4\beta + \lambda_2 \sin^4\beta + \frac{\lambda}{2}\sin^2 2\beta\right) v^2 & \left(\lambda_2 \sin^2\beta - \lambda_1 \cos^2\beta + \lambda\cos 2\beta\right)\frac{\sin 2\beta}{2} v^2 \\ \left(\lambda_2 \sin^2\beta - \lambda_1 \cos^2\beta + \lambda\cos 2\beta\right)\frac{\sin 2\beta}{2} v^2 & M^2 + (\lambda_1 + \lambda_2 - 2\lambda)\frac{\sin^2 2\beta}{4} v^2 \end{bmatrix}, \tag{7}$$

for CP-even Higgs bosons,

$$M_A^2 = M^2 - \lambda_5 v^2, \tag{8}$$

for CP-odd Higgs boson, and

$$M_S^2 = \begin{bmatrix} M^2 - \frac{\lambda_4+\lambda_5}{2} v^2 & -\frac{\mu v}{\sqrt{2}} \\ -\frac{\mu v}{\sqrt{2}} & m_0^2 + \left(\frac{\sigma_1}{2}\cos^2\beta + \frac{\sigma_2}{2}\sin^2\beta\right) v^2 \end{bmatrix}, \tag{9}$$

for charged Higgs bosons. Here, $\lambda \equiv \lambda_3 + \lambda_4 + \lambda_5$ and $M^2 \equiv m_3^2/\sin\beta\cos\beta$. The vacuum expectation value v ($\sim$ 246 GeV) is equal to $\sqrt{2}\sqrt{\langle\phi_1^0\rangle^2 + \langle\phi_2^0\rangle^2}$. Mass eigenstates for the CP-even and the charged Higgs bosons are obtained by diagonalizing the mass matrices (7) and (9), respectively. The original Higgs boson fields, ϕ_1, ϕ_2, ω^-, can be expressed in terms of the physical states and the Nambu-Goldstone modes (G^0 and $G^\pm$) as

---

[2]Our analyses will thus be valid in the cases where the effect of the bottom Yukawa coupling is sufficiently small; i.e. in the region of not too large $\tan\beta$.

$$\phi_1^0 = \frac{1}{\sqrt{2}}\Big(v\cos\beta + H\cos\alpha - h\sin\alpha + i(G^0\cos\beta - A\sin\beta)\Big)\,, \tag{10}$$

$$\phi_1^- = G^-\cos\beta - (S_1^-\cos\chi - S_2^-\sin\chi)\sin\beta, \tag{11}$$

$$\phi_2^0 = \frac{1}{\sqrt{2}}\Big(v\sin\beta + H\sin\alpha + h\cos\alpha + i(G^0\sin\beta + A\cos\beta)\Big)\,, \tag{12}$$

$$\phi_2^- = G^-\sin\beta + (S_1^-\cos\chi - S_2^-\sin\chi)\cos\beta, \tag{13}$$

$$\omega^- = S_1^-\sin\chi + S_2^-\cos\chi\,, \tag{14}$$

where the angle α and χ are defined from the matrices which diagonalize the 2×2 matrices M_N^2 and M_S^2, respectively. Namely, we have

$$\begin{pmatrix} \cos(\alpha-\beta) & \sin(\alpha-\beta) \\ -\sin(\alpha-\beta) & \cos(\alpha-\beta) \end{pmatrix} M_N^2 \begin{pmatrix} \cos(\alpha-\beta) & -\sin(\alpha-\beta) \\ \sin(\alpha-\beta) & \cos(\alpha-\beta) \end{pmatrix} = \begin{pmatrix} m_H^2 & 0 \\ 0 & m_h^2 \end{pmatrix}, \tag{15}$$

$$\begin{pmatrix} \cos\chi & \sin\chi \\ -\sin\chi & \cos\chi \end{pmatrix} M_S^2 \begin{pmatrix} \cos\chi & -\sin\chi \\ \sin\chi & \cos\chi \end{pmatrix} = \begin{pmatrix} m_{S_1}^2 & 0 \\ 0 & m_{S_2}^2 \end{pmatrix}, \tag{16}$$

where $m_H^2 > m_h^2$ and $m_{S_1}^2 > m_{S_2}^2$. The mixing angles α and χ then satisfy

$$\tan 2\alpha = \frac{M^2 - (\lambda_3+\lambda_4+\lambda_5)\,v^2}{M^2 - (\lambda_1\cos^2\beta - \lambda_2\sin^2\beta)\frac{v^2}{\cos 2\beta}}\ \tan 2\beta, \tag{17}$$

$$\tan 2\chi = \frac{-\sqrt{2}\mu v}{M^2 - m_0^2 - \Big(\lambda_4+\lambda_5+\sigma_1\cos^2\beta + \sigma_2\sin^2\beta\Big)\frac{v^2}{2}}\,, \tag{18}$$

which show that α and χ approaches to $\beta - \frac{\pi}{2}$ and zero, respectively[3], when M^2 is much greater than v^2, μ^2 and m_0^2; i.e., in the decoupling regime. In this limit, the massive Higgs bosons from the extra weak-doublet are very heavy due to the large M so that they are decoupled from the low energy observable.

Although neutrinos in this model are massless at the tree level, the loop diagrams involving charged Higgs bosons, as shown in Fig. 1, can generate the Majorana mass terms for all three-flavors of neutrinos. It was shown [2] that at the one-loop order, the neutrino mass matrix, defined in the basis where the charged lepton Yukawa-coupling constants are

[3]Recall that we assumed $m_H > m_h$.

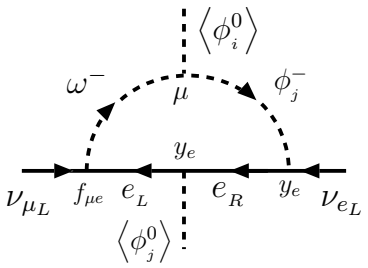

FIG. 1. A representative diagram that generates the neutrino mass. For type-I, $i = 1$, $j = 2$, and for type-II, $i = 2$, $j = 1$.

diagonal in the lepton flavor space, is real and symmetric with vanishing diagonal elements. More explicitly, we have

$$M_\nu = \begin{pmatrix} 0 & m_{12} & m_{13} \\ m_{12} & 0 & m_{23} \\ m_{13} & m_{23} & 0 \end{pmatrix} , \tag{19}$$

with

$$m_{ij} = f_{ij}(m_{e_j}^2 - m_{e_i}^2)\mu \cot\beta \frac{1}{16\pi^2} \frac{1}{m_{S_1}^2 - m_{S_2}^2} \ln \frac{m_{S_1}^2}{m_{S_2}^2} , \tag{20}$$

where m_{e_i} $(i = 1, 2, 3)$ is the charged lepton mass for type-I. For type-II, $\cot\beta$ should be replaced by $\tan\beta$. Note that Eq. (20) is valid for $m_{S_i} \gg m_{e_j}$.

The phenomenological analysis of the above mass matrix was given in Ref. [4,5]. It was concluded that, in the Zee-model, the bi-maximal mixing solution is the only possibility to reconcile the atmospheric and the solar neutrino data. Here we give a brief summary of their results, for completeness. Let us denote the three eigenvalues for the neutrino mass matrix, cf. Eq. (19), as m_{ν_1}, m_{ν_2} and m_{ν_3}, which satisfy $m_{\nu_1} + m_{\nu_2} + m_{\nu_3} = 0$. The possible pattern of the neutrino mass spectrum which is allowed in the Zee-model is $|m_{\nu_1}| \simeq |m_{\nu_2}| \gg |m_{\nu_3}|$, with $m_{\nu_1}^2 - m_{\nu_3}^2 \simeq m_{\nu_2}^2 - m_{\nu_3}^2 = \Delta m_{atm}^2$, and $\left| m_{\nu_1}^2 - m_{\nu_2}^2 \right| = \Delta m_{solar}^2$, where $\Delta m_{atm}^2 = O(10^{-3})$ eV^2 from the atmospheric neutrino data, and $\Delta m_{solar}^2 = O(10^{-5})$ eV^2 (MSW large angle solution) or $O(10^{-10})$ eV^2 (vacuum oscillation solution) from the solar neutrino data[4]. Thus,

[4]Due to the structure of the mass matrix, cf. Eq. (19), only the hierarchy pattern $|m_{\nu_1}| \simeq |m_{\nu_2}| \gg$

we have $|m_{\nu_1}| \simeq |m_{\nu_2}| \simeq \sqrt{\Delta m^2_{atm}}$ ($m_{\nu_1} \simeq -m_{\nu_2}$) and $|m_{\nu_3}| \simeq \frac{\Delta m^2_{solar}}{2\sqrt{\Delta m^2_{atm}}}$. The approximate form of the neutrino mass matrix is given by

$$M_\nu = \begin{pmatrix} 0 & \pm\sqrt{\frac{|m_{\nu_1} m_{\nu_2}|}{2}} & \mp\sqrt{\frac{|m_{\nu_1} m_{\nu_2}|}{2}} \\ \pm\sqrt{\frac{|m_{\nu_1} m_{\nu_2}|}{2}} & 0 & -m_{\nu_1} - m_{\nu_2} \\ \mp\sqrt{\frac{|m_{\nu_1} m_{\nu_2}|}{2}} & -m_{\nu_1} - m_{\nu_2} & 0 \end{pmatrix}, \tag{21}$$

where the upper (lower) sign corresponds to $m_{\nu_1} < 0$ (> 0) case, and the corresponding Maki-Nakagawa-Sakata (MNS) matrix [18] which diagonalizes the neutrino mass matrix is

$$U = \begin{pmatrix} \sqrt{\frac{|m_{\nu_2}|}{|m_{\nu_1}|+|m_{\nu_2}|}} & \sqrt{\frac{|m_{\nu_1}|}{|m_{\nu_1}|+|m_{\nu_2}|}} & 0 \\ -\frac{1}{\sqrt{2}}\sqrt{\frac{|m_{\nu_1}|}{|m_{\nu_1}|+|m_{\nu_2}|}} & \frac{1}{\sqrt{2}}\sqrt{\frac{|m_{\nu_2}|}{|m_{\nu_1}|+|m_{\nu_2}|}} & \frac{1}{\sqrt{2}} \\ \frac{1}{\sqrt{2}}\sqrt{\frac{|m_{\nu_1}|}{|m_{\nu_1}|+|m_{\nu_2}|}} & -\frac{1}{\sqrt{2}}\sqrt{\frac{|m_{\nu_2}|}{|m_{\nu_1}|+|m_{\nu_2}|}} & \frac{1}{\sqrt{2}} \end{pmatrix}, \tag{22}$$

In the above equations, we took the limiting case where $U_{13} = 0$ and $U_{32} = U_{23} = \frac{1}{\sqrt{2}}$ [5]. From Eqs. (20) and (21), we obtain

$$\left|\frac{f_{12}}{f_{13}}\right| \simeq \frac{m_\tau^2}{m_\mu^2} \simeq 3 \times 10^2, \tag{23}$$

$$\left|\frac{f_{13}}{f_{23}}\right| \simeq \frac{\sqrt{2}\Delta m^2_{atm}}{\Delta m^2_{solar}} \simeq \begin{cases} 10^2 & \text{(for the MSW large angle solution)} \\ 10^7 & \text{(for the vacuum oscillation solution)} \end{cases}. \tag{24}$$

Therefore, the magnitudes of the three coupling constants should satisfy the relation $|f_{12}| \gg |f_{13}| \gg |f_{23}|$. This hierarchy among the couplings f_{ij} is crucial for our later discussion on the phenomenology of the singlet charged Higgs bosons.

For a given value of the parameters m_{S_1}, m_{S_2}, $\tan\beta$ and μ, the coupling constants f_{ij} can be calculated from Eq. (20). For example, for $m_{S_1} = 500\,\text{GeV}$, $m_{S_2} = 100\,\text{GeV}$, $\tan\beta = 1$, $\mu = 100\,\text{GeV}$ and $m_{12} = 3 \times 10^{-2}\,\text{eV}$, we obtain $|f_{12}| \sim 3 \times 10^{-4}$. As in this example, when

---

$|m_{\nu_3}|$, rather than $|m_{\nu_1}| \simeq |m_{\nu_2}| \ll |m_{\nu_3}|$, is realized in the Zee-model [4,5]

[5] This limit corresponds to $\theta_2 = \frac{\pi}{4}$ and $\theta_3 = 0$ in the notation of Ref. [18].

S_1^- is rather heavy and the lighter charged Higgs boson S_2^- is almost a weak singlet, i.e. the mixing angle χ approaches to zero, it is unlikely that there are observable effects to the low energy data [7]; e.g., the muon life-time, the universality of tau decay into electron or muon, the rare decay of $\mu \to e\gamma$, the universality of W-boson decay into electron, muon or tau, and the decay width of Z boson. When $|f_{ij}|$ are small, we do not expect a large rate in the lepton flavor violation decay of a light neutral Higgs boson, such as $h \to \mu^\pm e^\mp$ (the largest one), $h \to e^\pm \tau^\mp$, or $h \to \mu^\pm \tau^\mp$ (the smallest one). On the contrary, as to be discussed in Section IV, the decay width of $h \to \gamma\gamma$ can significantly deviate from the SM value.

Finally, the phenomenological constraints on f_{12} were derived in Ref. [6]. From the consistency of the muon decay rate and electroweak precision test it was found that

$$\frac{f_{12}^2}{\overline{M}^2} < 7 \times 10^{-4} G_F \,, \tag{25}$$

where G_F is the Fermi constant, and

$$\frac{1}{\overline{M}^2} = \frac{\sin^2\chi}{m_{S_1}^2} + \frac{\cos^2\chi}{m_{S_2}^2}. \tag{26}$$

This means that the f_{ij} cannot be $O(1)$ unless the charged Higgs boson masses are at the order of 10 TeV.

III. HIGGS BOSON MASS AND COUPLINGS THROUGH RGE'S

In this section, we determine the bounds on the mass of the lightest CP-even Higgs boson as a function of the cut-off scale of the Zee-model by analyzing the set of renormalization group equations (RGE's). We also study the allowed ranges of the coupling constants, especially σ_1 and σ_2 in Eq. (4). In Sec. IV, they will be used to evaluate how much the partial decay width of $h \to \gamma\gamma$ can deviate from its SM value due to the one-loop contribution from the singlet charged Higgs boson.

The mass bounds are determined in the following manner. For each set of parameters defined at the electroweak scale, the running coupling constants are calculated numerically

through RGE's at the one-loop level. We require that all the dimensionless coupling constants do not blow up below a given cut-off scale Λ, and the coupling constants satisfy the vacuum stability condition. We vary the input parameters at the electroweak scale and determine the possible range of the lightest CP-even Higgs boson mass as a function of Λ. In a similar manner, we also study the allowed ranges of various Higgs boson self-coupling constants at the electroweak scale as well as a function of the lightest CP-even Higgs boson mass.

We derived the one-loop RGE's for the Zee-model, and listed them in the Appendix for reference. For simplicity, in the RGE's, we have neglected all the Yukawa coupling constants (y_u, y_d, y_e) but the top Yukawa coupling y_t.[6] Although we kept the new coupling constants f_{ij} in the RGE's listed in the Appendix, we have neglected f_{ij} in the numerical calculation. This is because the magnitudes of these coupling constants are numerically too small to affect the final results unless the singlet-charged scalar-boson mass is larger than a few TeV [cf. Eq. (25)]. The dimensionless coupling constants relevant to our numerical analysis are the three gauge-coupling constants g_1, g_2, g_3, the top Yukawa-coupling constant y_t, and eight scalar self-coupling constants, λ_i ($i = 1 - 5$) and σ_i ($i = 1 - 3$). There are five dimensionful parameters in the Higgs potential, namely m_1^2, m_2^2, m_3^2, m_0^2 and μ. Instead of m_1^2, m_2^2, m_3^2, we take v, $\tan\beta$, and $M^2 \equiv m_3^2/\sin\beta\cos\beta$, as independent parameters, where v (~ 246 GeV) characterizes the weak scale and M the soft-breaking scale of the discrete symmetry.

In the actual numerical calculation we first fix $\tan\beta$ and M. For a given mass (m_h) of the lightest CP-even Higgs boson, we solve one of the λ_i, which is chosen to be λ_3 here, in terms of other λ_i. We then numerically evaluate all dimensionless coupling constants according to the RGE's. From m_h to M we use the SM RGE's, which are matched to the

[6] In the model with the type-II Yukawa interaction, the bottom-quark Yukawa interaction can become important for a large $\tan\beta$.

Zee-model RGE's at the soft-breaking scale M. [7]

We requires the following two conditions to be satisfied for each scale Q up to a given cut-off scale Λ.

1. Applicability of the perturbation theory implies

$$\lambda_i(Q) < 8\pi, \quad \sigma_i(Q) < 8\pi, \quad y_t^2(Q) < 4\pi\,. \tag{27}$$

2. The vacuum stability conditions must be satisfied. The requirement that quartic coupling terms of the scalar potential do not have a negative coefficient in any direction leads to the following conditions at each renormalization scale Q:

   (a)

$$\lambda_1(Q) > 0, \quad \lambda_2(Q) > 0, \quad \sigma_3(Q) > 0\,. \tag{28}$$

   (b)

$$\sigma_1(Q) + \sqrt{\frac{\lambda_1(Q)\,\sigma_3(Q)}{2}} > 0\,, \tag{29}$$

$$\sigma_2(Q) + \sqrt{\frac{\lambda_2(Q)\,\sigma_3(Q)}{2}} > 0\,, \tag{30}$$

$$\overline{\lambda}(Q) + \sqrt{\lambda_1(Q)\,\lambda_2(Q)} > 0\,, \tag{31}$$

   where $\overline{\lambda}(Q) = \lambda_3(Q) + \min\left(0,\ \lambda_4(Q) + \lambda_5(Q),\ \lambda_4(Q) - \lambda_5(Q)\right)$.

---

[7] The parameter m_0 and μ are only relevant to the charged scalar mass matrix. In principle, our numerical results also depend on these parameters through the renormalization of various coupling constants from the scale of m_h to the charged scalar mass. Since these effects are expected to be small, we calculate the RGE's as if all the scalar-bosons except h decouple at the scale M.

(c) If $\sigma_1(Q) < 0$ and $\sigma_2(Q) < 0$, then

$$\overline{\lambda}(Q) + \frac{2}{\sigma_3(Q)} \left\{ \sqrt{\left(\frac{\lambda_1(Q)\,\sigma_3(Q)}{2} - \sigma_1^2(Q) \right) \left(\frac{\lambda_2(Q)\,\sigma_3(Q)}{2} - \sigma_2^2(Q) \right)} - \sigma_1(Q)\,\sigma_2(Q) \right\} > 0\,. \tag{32}$$

If $\sigma_1(Q) < 0$ and $\overline{\lambda}(Q) < 0$, then

$$\sigma_2(Q) + \frac{1}{\lambda_1(Q)} \left\{ \sqrt{\left(\lambda_1(Q)\,\lambda_2(Q) - \overline{\lambda}^2(Q) \right) \left(\frac{\lambda_1(Q)\,\sigma_3(Q)}{2} - \sigma_1^2(Q) \right)} - \sigma_1(Q)\,\overline{\lambda}(Q) \right\} > 0\,. \tag{33}$$

If $\sigma_2(Q) < 0$ and $\overline{\lambda}(Q) < 0$, then

$$\sigma_1(Q) + \frac{1}{\lambda_2(Q)} \left\{ \sqrt{\left(\lambda_1(Q)\,\lambda_2(Q) - \overline{\lambda}^2(Q) \right) \left(\frac{\lambda_2(Q)\,\sigma_3(Q)}{2} - \sigma_2^2(Q) \right)} - \sigma_2(Q)\,\overline{\lambda}(Q) \right\} > 0\,. \tag{34}$$

[When $\sigma_1(Q)$, $\sigma_2(Q)$ and $\overline{\lambda}(Q)$ are all negative, the above three conditions are equivalent.]

In addition to the above conditions, we also demand local stability of the potential at the electroweak scale, namely, we calculate the mass spectrum of all scalar fields at the extremum of the potential and demand that all eigenvalues of the squared scalar mass are positive. We scan the remaining seven-dimensional space of λ_i and σ_i and examine whether a given mass of the lightest CP-even Higgs boson is allowed under the above conditions. In this way we obtain the allowed range of m_h as a function of $\tan\beta$ and M, for each value of the cut-off scale Λ.

First, we discuss our result in the decoupling case, in which the soft-breaking scale M is much larger than the electroweak scale $\sim v$, and the masses of all the Higgs bosons but h (and S_2) are at the order of M [8]. In Fig. 2, the allowed range of m_h is shown as a function of $\tan\beta$ for $M = 1000$ GeV. (We take the pole mass of top quark $m_t = 175$ GeV,

[8] In the decoupling regime ($M \to \infty$, which leads to $\alpha \to \beta - \frac{\pi}{2}$ and $\chi \to 0$), the masses of h and S_2 are dominated by the (11) component of the mass matrix in Eq. (7) and the (22) component of that in Eq. (9), respectively. The mass of h is determined by the self-coupling constants λ_i, while that of S_2 depends not only on the self-couplings constants σ_i but also on the free mass parameter m_0. As noticed in the footnote 7, from m_h to M, the SM RGE are used in our analysis, even if

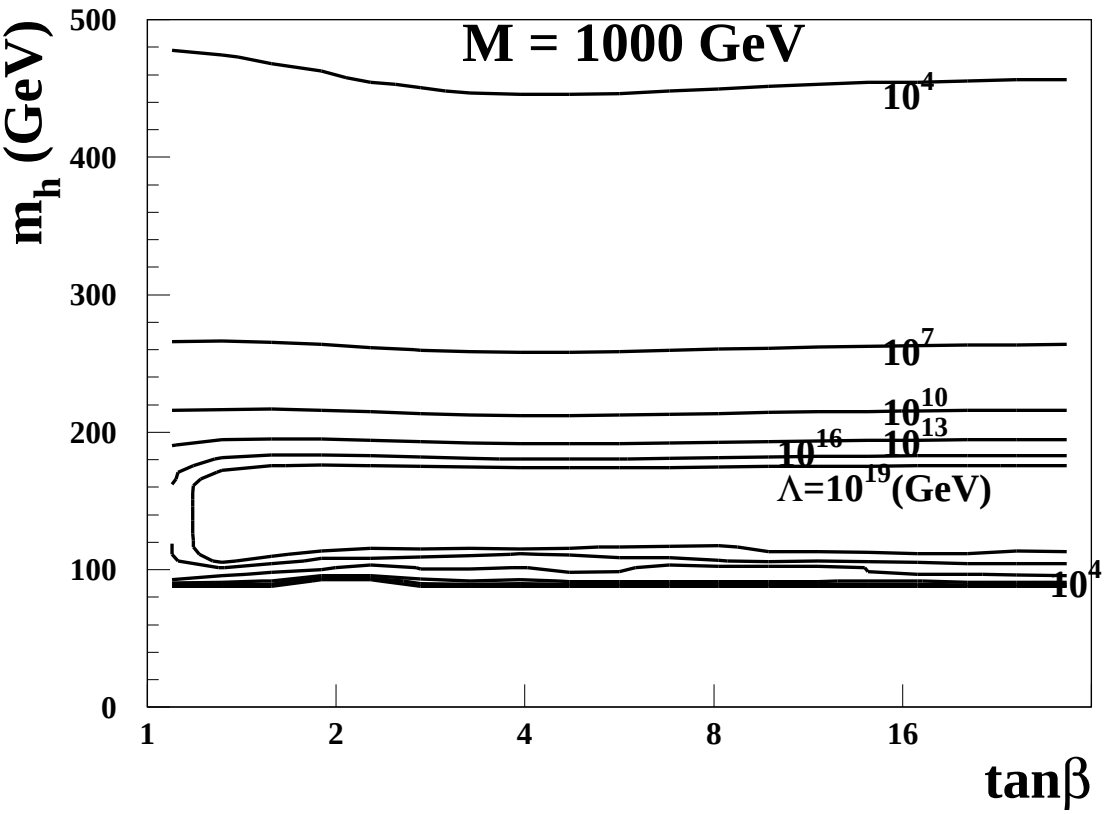

FIG. 2. The allowed mass range of the lightest CP-even Higgs boson for $M = 1000$ GeV. Λ is the cut-off scale.

$\alpha_s(m_Z) = 0.118$ for numerical calculation.) The allowed ranges are shown as contours for six different values of Λ, i.e. $\Lambda = 10^{19}$, 10^{16},10^{13},10^{10},10^7 and 10^4 GeV. For most values of $\tan\beta$, except for small $\tan\beta$ region, the upper bound of m_h is about 175 GeV and the lower bound is between 110 GeV and 120 GeV for the cut-off scale Λ to be near the Planck scale. The numerical values in this figure are very close to those in the corresponding figure for the THDM discussed in Ref. [13]. Compared to the corresponding lower mass bound in the SM, which is 145 GeV when using the one-loop RGE's, the lower mass bound in this model is reduced by about 30 GeV to 40 GeV. The reason is similar to the THDM case: the lightest CP-even Higgs boson mass is essentially determined by the value of λ_2 for $\tan\beta$ to

---

the mass of S_2 is smaller than M. The effect of S_2 on the mass bound of h is expected to be small, because at the one-loop level the primary effect is through the running of g_1, whose contribution to the right-handed side of the RGE for the Higgs-self coupling constant is small.

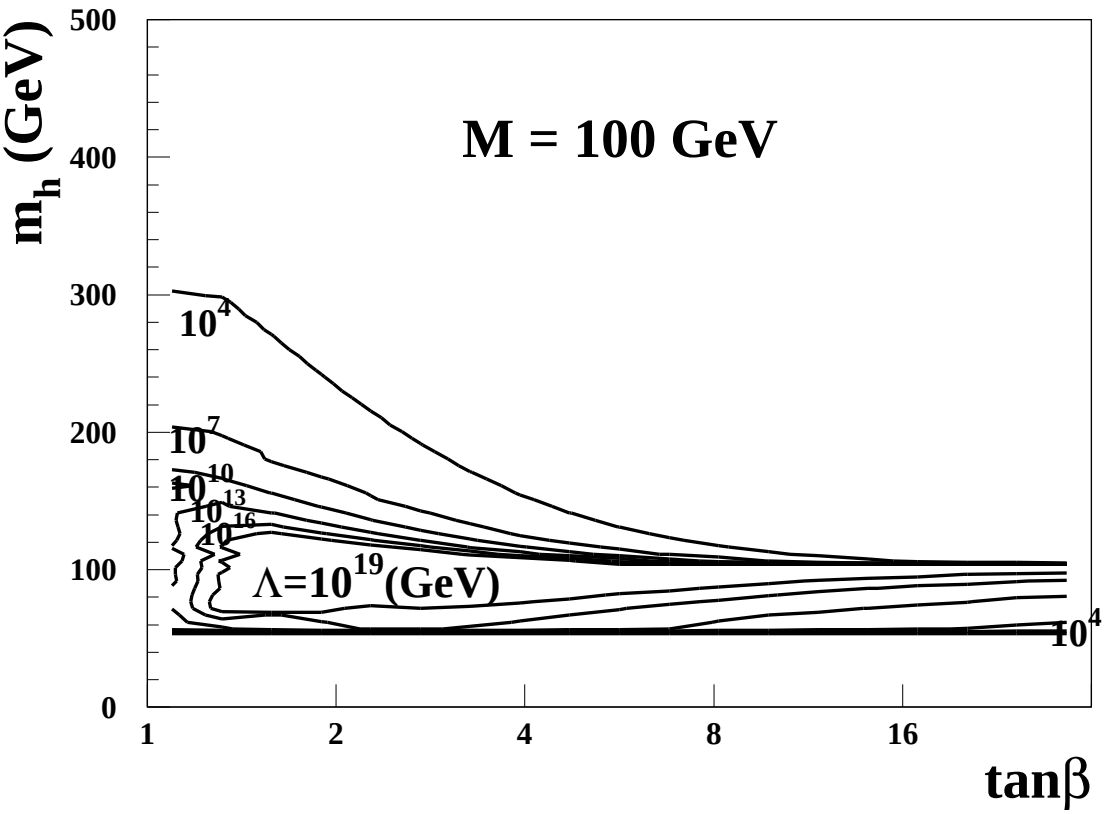

FIG. 3. The allowed mass range of the lightest CP-even Higgs boson for $M = 100$ GeV.

be larger than about 2 , where λ_2 plays the role of the self-coupling constant of the Higgs potential in the SM[9]. On the right-hand side of the RGE for λ_2, cf. Eq. (A5), there are additional positive-definite terms $\frac{2}{16\pi^2}\left(\lambda_3^2 + (\lambda_3+\lambda_4)^2 + \lambda_5^2 + \sigma_2^2\right)$ as compared to the RGE for the Higgs self-coupling constant in the SM. These additional terms can improve vacuum stability, and allow lower values of m_h. Therefore, one of the features of the model is to have a different mass range for the lightest CP-even Higgs boson as compared to the SM Higgs boson, for a given cut-off scale.

Next, we show our result for M to be around v. In Fig. 3, we present the m_h bound for $M = 100$ GeV. In this case, the allowed range of m_h is reduced as compared to that in the decoupling case, and lies around $m_h \sim M$ for large $\tan\beta$. Notice that we have not included

[9]However, $\tan\beta$ cannot be too large to ignore the contribution of the bottom quark in the case with the type-II Yukawa interaction.

phenomenological constraints from the $b \to s\gamma$, ρ parameter and the direct Higgs boson search experiment at LEP. As mentioned before, the mass bounds obtained from the RGE analysis are the same for the type-I and type-II models without these phenomenological constraints. However, it was shown in Ref. [13] that the $b \to s\gamma$ data can put a strong constraint on the allowed range of the Higgs boson mass for $M \lesssim 200$–400 GeV in the type-II THDM, whereas there is no appreciable effect in the type-I model. This is because a small M implies a light charged Higgs boson in the THDM which can induce a large decay branching ratio for $b \to s\gamma$ in the type-II model [19][10]. We expect a similar constraint from the $b \to s\gamma$ data on the type-II Zee-model, when M is small.

In Fig. 4, we show the upper and lower bounds of m_h as a function of M for various values of Λ. For given M, we scan the range of $\tan\beta$ for $1 \leq \tan\beta \leq 16\sqrt{2}$ ($\simeq 22.6$). We find that the obtained m_h bounds are almost the same as those for the THDM. The primary reason for this is that the new coupling constants σ_1, σ_2 and σ_3 do not appear directly in the mass formula for m_h, and therefore, do not induce large effects on the bounds of m_h.

We also investigate the allowed range of coupling constants σ_1, σ_2 and σ_3. For this purpose, we fix σ_1 (or σ_2, σ_3) as well as $\tan\beta$ and M to evaluate the upper and the lower bounds of m_h for each Λ value. In this way, we determine the possible range of σ_1 (or σ_2, σ_3) under the condition that the theory does not break down below the cut-off scale Λ. In Fig. 5, we present the allowed range of σ_1 and m_h for different choice of Λ in the case of $M = 1000$ GeV and $\tan\beta = \sqrt{2}$ or $16\sqrt{2}$. A similar figure is shown for the possible range of σ_2 in Fig. 6. We see that the maximal value of σ_1 and σ_2 is around 0.7 for $m_h = 110 - 170$ GeV if we take the cut-off scale to be 10^{19} GeV. For smaller value of Λ the allowed ranges of σ_i becomes larger. For example, σ_1 can exceed 1 for $\Lambda = 10^{13}$ GeV. We have calculated for other value of $\tan\beta$ and checked that these figures does not change greatly between

[10]In addition, it has been known that the R_b data also give strong constraints on the charged Higgs bosons in the type-II THDM [20].

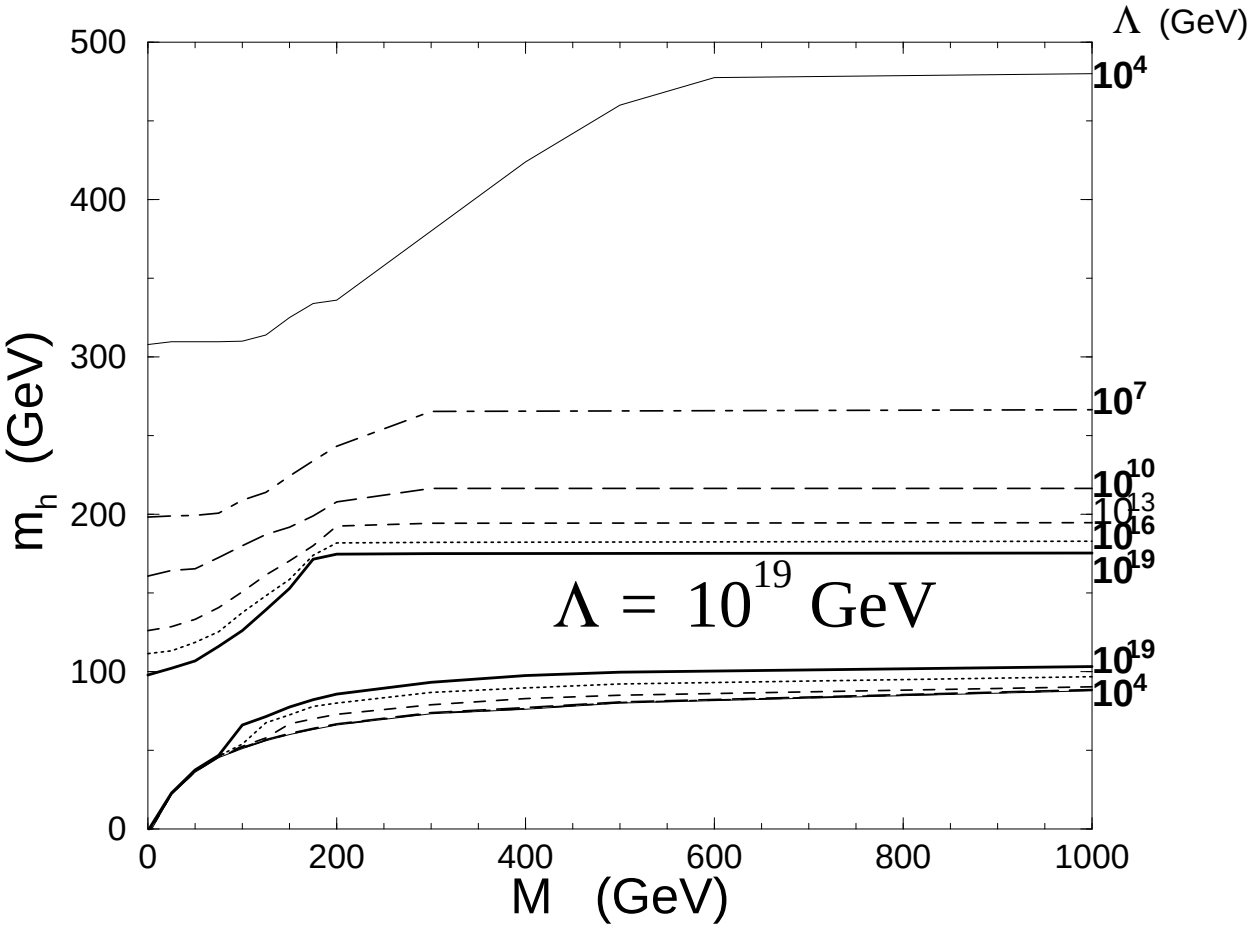

FIG. 4. The allowed ranges of the lightest CP-even Higgs boson mass as a function of M for various Λ values.

$\tan\beta = 1.4$ and $16\sqrt{2}$. We also present the allowed range in the σ_1 and σ_2 plane for a fixed value of m_h in Figs. 7 and 8 for $m_h = 125$ GeV and $m_h = 140$ GeV, respectively. For either value of m_h with $\tan\beta = 16\sqrt{2}$, both σ_1 and σ_2 can be as large as 0.5 (2) for $\Lambda = 10^{19}$ (10^7) GeV. The allowed range of σ_3 and m_h for various values of Λ is given in Fig. 9. It is shown that, σ_3 has to be larger than zero, due to the vacuum stability condition. The maximal value of σ_3 is about 1 (3) for $\Lambda = 10^{19}$ (10^7) GeV and $M = 1000$ GeV. The impact of these new coupling constants on the collider phenomenology is discussed in the next section.

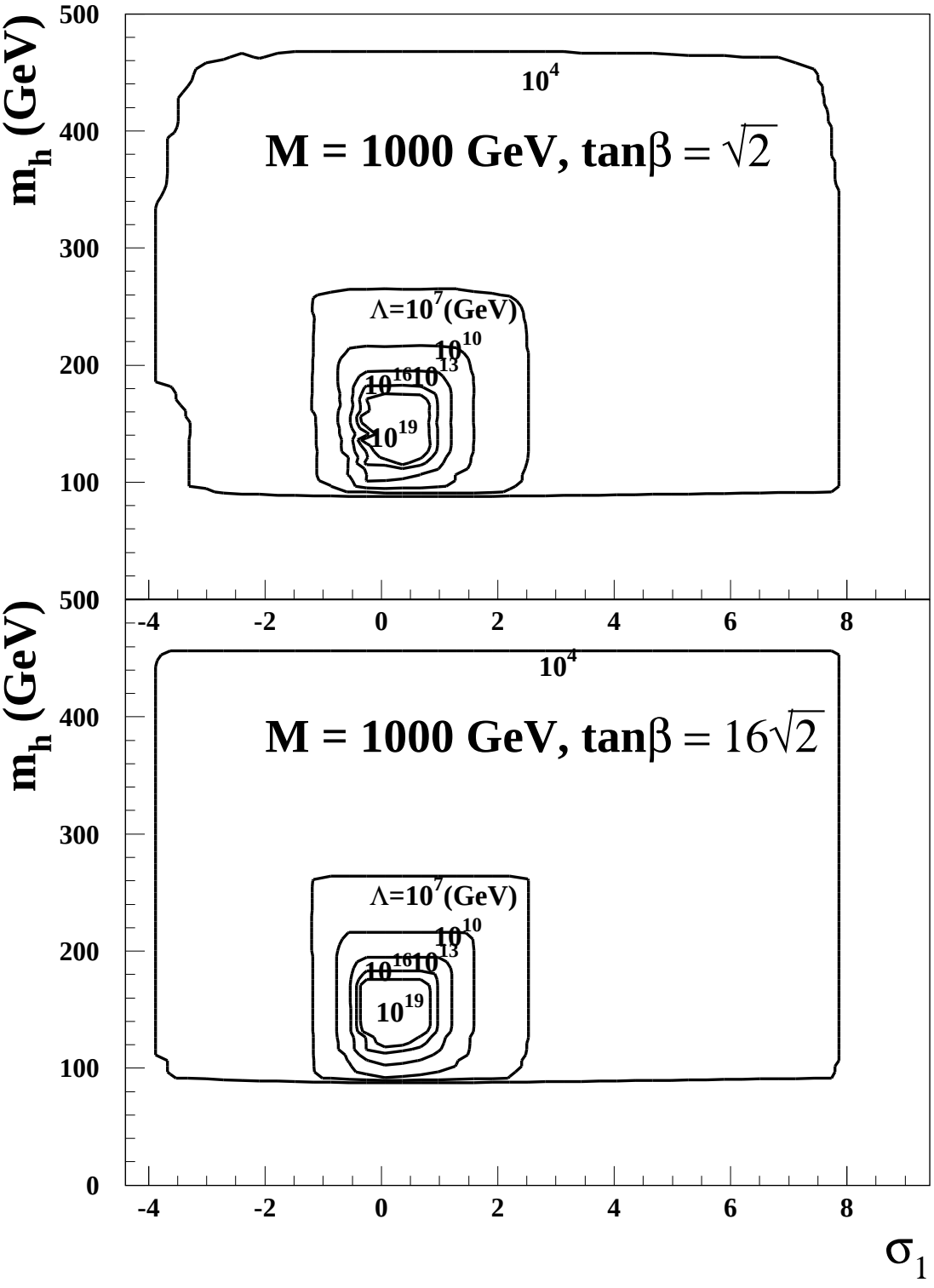

FIG. 5. The allowed range of σ_1 and m_h for various Λ values.

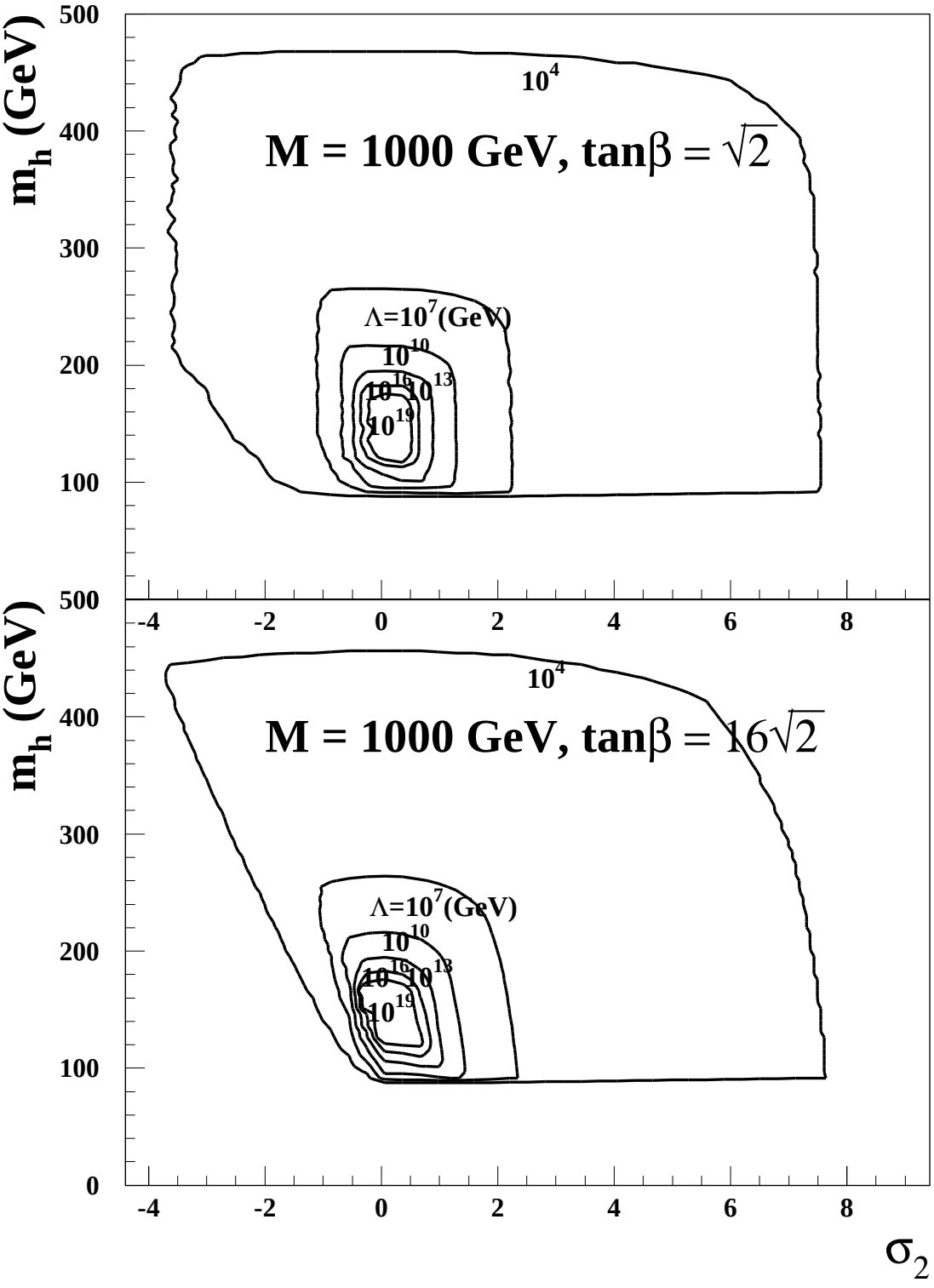

FIG. 6. The allowed range of σ_2 and m_h for various Λ values.

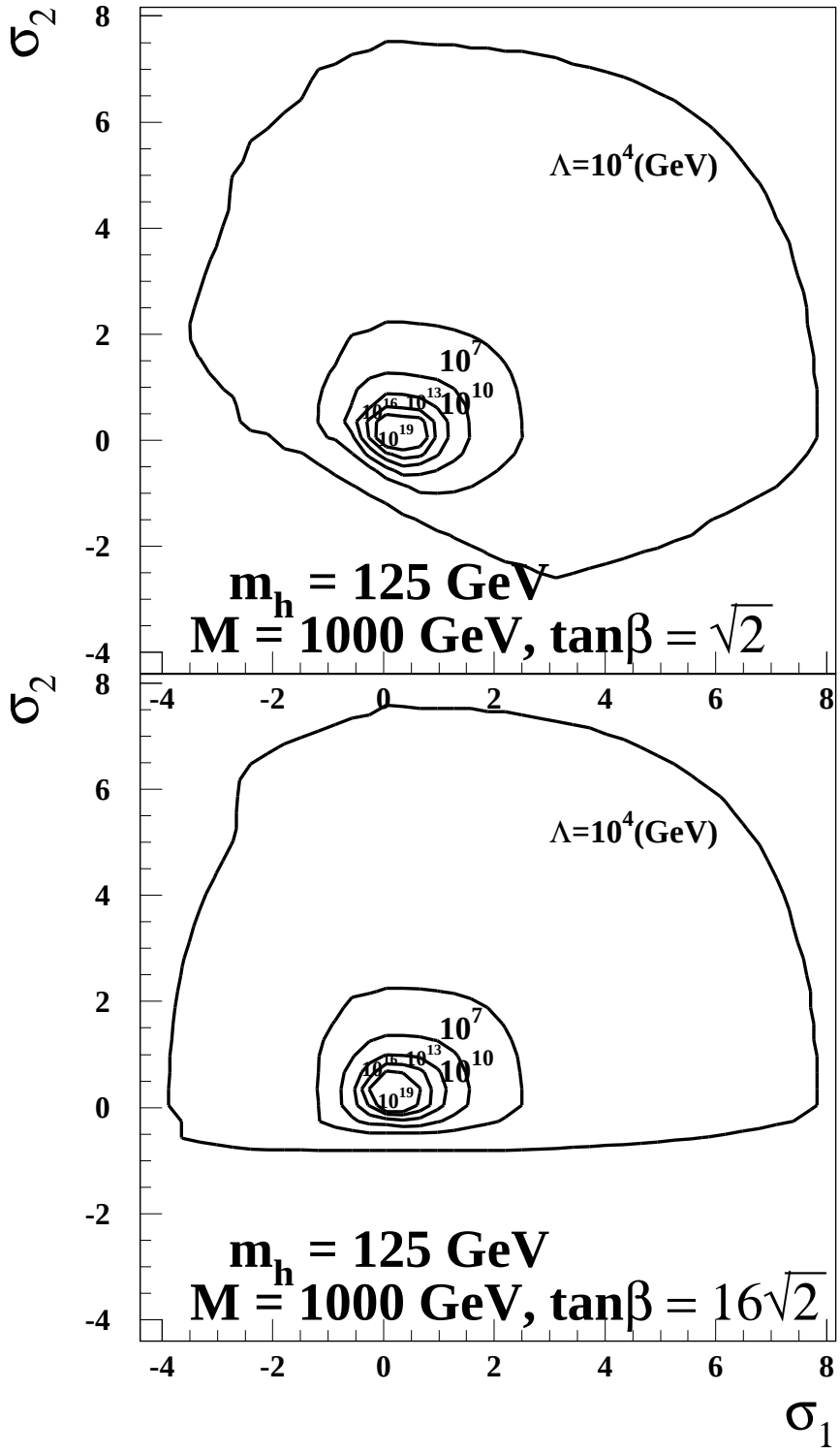

FIG. 7. The allowed range of σ_1 and σ_2 for $m_h = 125$ GeV.

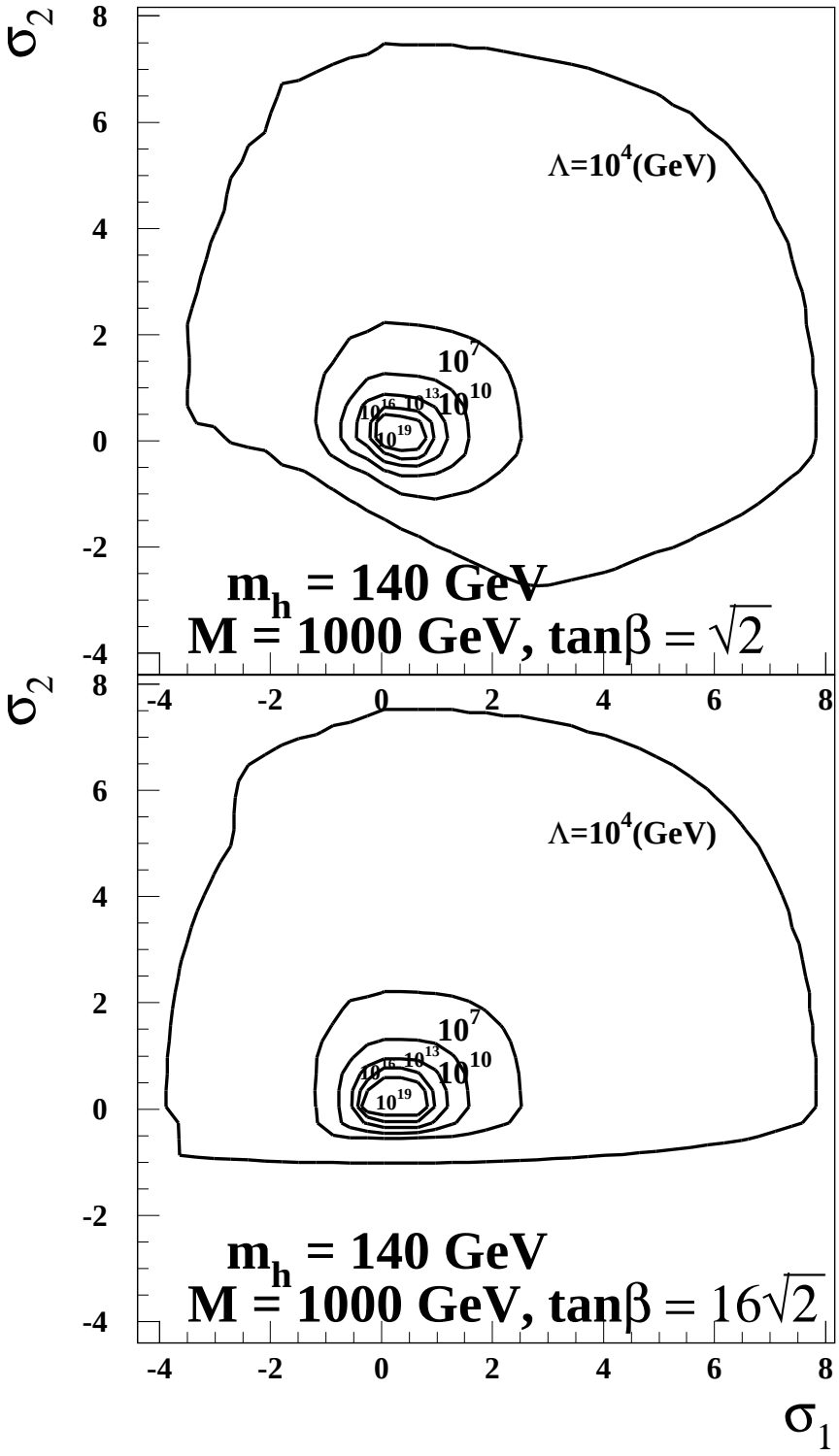

FIG. 8. The allowed range of σ_1 and σ_2 for $m_h = 140$ GeV.

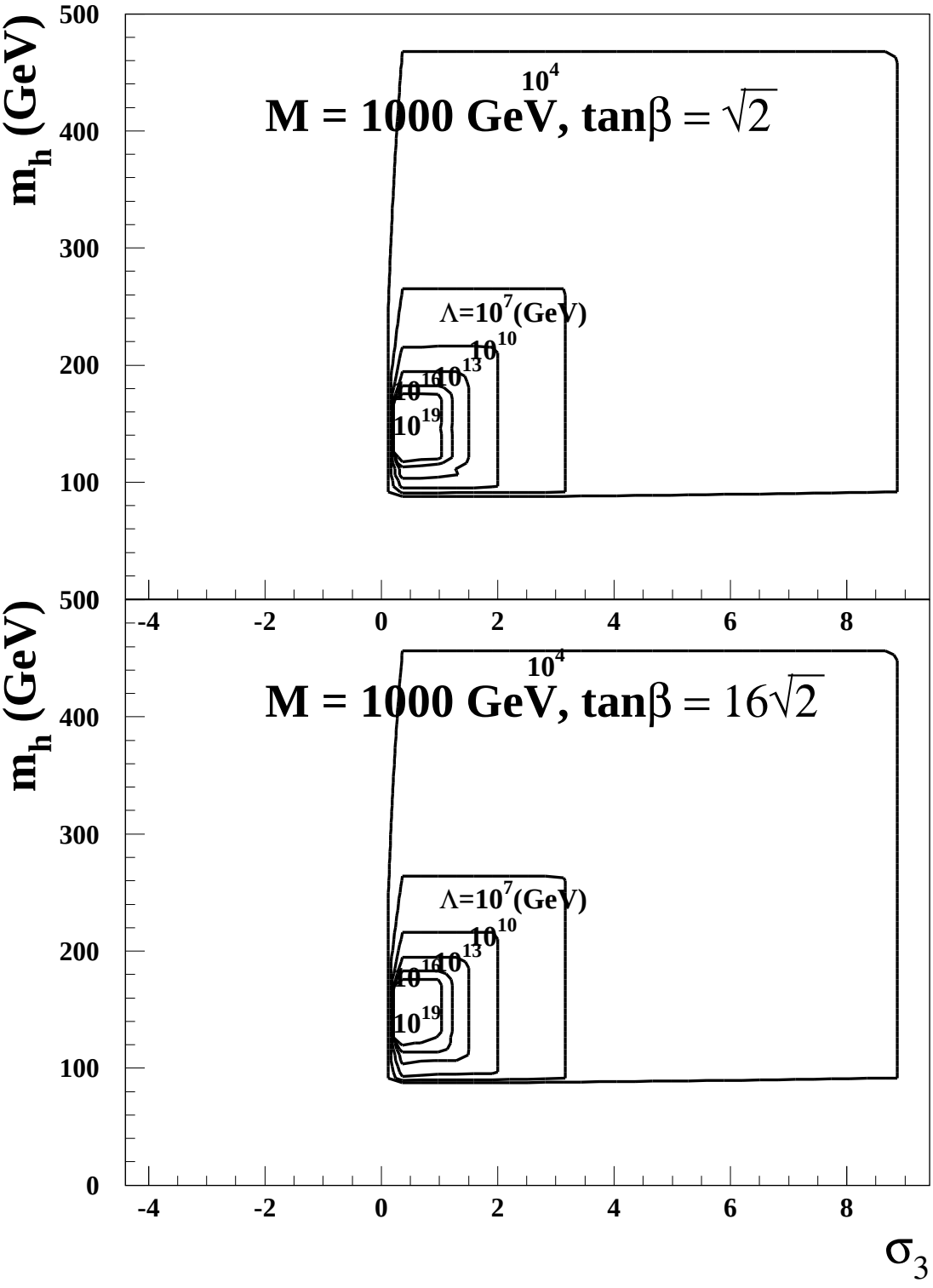

FIG. 9. The allowed range of σ_3 and m_h for various Λ values.

IV. TWO-PHOTON DECAY WIDTH OF THE NEUTRAL HIGGS BOSON

In this section, we study the phenomenological consequences of the Higgs boson mass and the Higgs-boson-coupling constants derived in the previous section. The important feature of the Higgs sector of the Zee-model is that there are an additional weak doublet and a singlet charged Higgs boson. The physical states of the Higgs particles are two CP-even Higgs bosons, one CP-odd Higgs boson and two pairs of charged Higgs bosons. Therefore, the Higgs phenomenology is quite close to the ordinary two-Higgs-doublet model. One unique difference is the existence of the additional weak-singlet charged Higgs boson. The effect of this extra charged Higgs boson is especially important when M is much larger than the Z boson mass, i.e. in the decoupling regime. In such a case, the heavier CP-even Higgs boson, the CP-odd Higgs boson as well as one of the charged Higgs bosons have masses approximately equal to M, and these heavy states are decoupled from low energy observables. (Note that the condition on the applicability of the perturbation theory forbids too large self-couplings among the Higgs bosons. Hence, in the limit of large M, the heavy Higgs bosons decouple from the low energy effective theory.) The remaining light states are the lighter CP-even Higgs boson h and the lighter charged Higgs boson S_2 which mainly comes from the weak-singlet. In the previous section, we show that, even in the decoupling case, there can be large difference in the allowed range of m_h between the Zee-model and the SM. Similarly, we expect that, even in the decoupling case, the presence of the additional weak-singlet charged Higgs boson can give rise to interesting Higgs phenomenology.

Since the lighter charged Higgs boson S_2 can couple to Higgs bosons and leptons, it can affect the decay and the production of the neutral Higgs bosons at colliders through radiative corrections. In the following, we consider the decay width of $h \to \gamma\gamma$ as an example. For a SM Higgs boson, the partial decay width (or branching ratio) of $h \to \gamma\gamma$ is small: ~ 9.2 keV (or 2.2×10^{-3}) for $m_h = 125$ GeV, and ~ 15.4 keV (or 1.9×10^{-3}) for $m_h = 140$ GeV, with a 175 GeV top quark. Nevertheless, it is an important discovery mode of the Higgs boson at the LHC experiments for m_h less than twice of the W-boson mass. Needless to

say that a change in the branching ratio of $h \to \gamma\gamma$ would lead to a different production rate of $pp \to hX \to \gamma\gamma X$. At future e^+e^- LC's, the branching ratio of $h \to \gamma\gamma$ can be determined via the reaction $e^+e^- \to q\overline{q}\gamma\gamma$ and $e^+e^- \to \nu\overline{\nu}\gamma\gamma$ with a 16-22% accuracy [16]. At the photon-photon collision option of the future LC's, the partial decay width of $h \to \gamma\gamma$ can be precisely tested within a 2 % accuracy [17] by measuring the inclusive production rate of the Higgs boson h. Clearly, a change in the partial decay width of $h \to \gamma\gamma$ will lead to a different production rate for h. In the Zee-model, such a change is expected after taking into account the loop contribution of the extra charged Higgs boson. We find that the deviation from the SM prediction can be sizable, and therefore testable at the LHC and future LC's.

The partial decay width of $h \to \gamma\gamma$ is calculated at the one-loop order. Similar to our previous discussion, we limit ourselves to the parameter space in which $1 \leq \tan\beta \leq 16\sqrt{2}$, and keep only the top quark contribution from the fermionic loop diagrams. Including the loop contributions from the W boson and the charged Higgs bosons S_1 and S_2 together with the top quark loop contribution, we obtain [21]

$$\Gamma(h \to \gamma\gamma) = \frac{(\alpha m_h)^3}{256\pi^2 \sin^2\theta_W m_W^2} \left| \sum_{i=S_1,S_2,t,W} I_i \right|^2 , \tag{35}$$

with

$$\begin{aligned} I_{S_1} &= R_{S_1} F_0(r_i) \,, \\ I_{S_2} &= R_{S_2} F_0(r_i) \,, \\ I_t &= \frac{4}{3}\left(\frac{\cos\alpha}{\sin\beta}\right) F_{1/2}(r_i) \,, \\ I_W &= \sin(\beta-\alpha) F_1(r_i) \,, \end{aligned}$$

where $r_i = \frac{4m_i^2}{m_h^2}$ and m_i is the mass of the internal lines in the loop diagram. R_{S_1} and R_{S_2} are given by

$$\begin{aligned} R_{S_1} = \frac{v^2}{2}\frac{1}{m_{S_1}^2}\Big[& \cos^2\chi \Big\{ -\lambda_1 \sin\alpha \sin^2\beta \cos\beta + \lambda_2 \cos\alpha \sin\beta \cos^2\beta \\ & + \lambda_3 \Big(\cos\alpha \sin^3\beta - \sin\alpha \cos^3\beta \Big) - \frac{1}{2}(\lambda_4+\lambda_5)\cos(\alpha+\beta)\sin 2\beta \Big\} \end{aligned}$$

$$+\sin^2\chi\left\{-\sigma_1\sin\alpha\cos\beta+\sigma_2\cos\alpha\sin\beta\right\}+\sqrt{2}\sin\chi\cos\chi\frac{\mu}{v}\sin(\alpha-\beta)\Big]\,, \tag{36}$$

$$\begin{aligned}R_{S_2}=\frac{v^2}{2}\frac{1}{m_{S_2}^2}\Big[&\sin^2\chi\left\{-\lambda_1\sin\alpha\sin^2\beta\cos\beta+\lambda_2\cos\alpha\sin\beta\cos^2\beta\right.\\&\left.+\lambda_3\left(\cos\alpha\sin^3\beta-\sin\alpha\cos^3\beta\right)-\frac{1}{2}(\lambda_4+\lambda_5)\cos(\alpha+\beta)\sin 2\beta\right\}\\&+\cos^2\chi\left\{-\sigma_1\sin\alpha\cos\beta+\sigma_2\cos\alpha\sin\beta\right\}-\sqrt{2}\sin\chi\cos\chi\frac{\mu}{v}\sin(\alpha-\beta)\Big]\,,\end{aligned} \tag{37}$$

and

$$F_0(r)=r\left(1-rf(r)\right)\,, \tag{38}$$

$$F_{1/2}(r)=-2r\left(1+(1-r)f(r)\right)\,, \tag{39}$$

$$F_1(r)=2+3r+3r\left(2-r\right)f(r)\,, \tag{40}$$

with

$$f(r)=\begin{cases}\left[\sin^{-1}\left(\sqrt{1/r}\right)\right]^2 & \text{if } r\geq 1\\ -\frac{1}{4}\left[\ln\frac{1+\sqrt{1-r}}{1-\sqrt{1-r}}-i\pi\right]^2 & \text{if } r<1\end{cases}\,. \tag{41}$$

In the decoupling case of the model, namely $M^2\gg\lambda_i v^2$, the above formulae are greatly simplified. This limit corresponds to $\alpha\to\beta-\frac{\pi}{2}$ and $\chi\to 0$, so that the light charged Higgs boson $S_2^\pm$ is identical to the weak-singlet Higgs boson $\omega^\pm$. Thus, we have

$$R_{S_2}\to\frac{v^2}{2}\frac{1}{m_{S_2}^2}\left(\sigma_1\cos^2\beta+\sigma_2\sin^2\beta\right)\,, \tag{42}$$

and both the top-quark and the W boson loop contributions reduce to their SM values. We like to stress that the weak-singlet Higgs boson does not directly couple to the quark fields in the limit of $\chi\to 0$. Therefore, it does not affect the decay rate of $b\to s\gamma$ at the one-loop order. Similarly, being a weak singlet, it also gives no contribution to the ρ parameter. Hence the low-energy constraint from either the $b\to s\gamma$ decay or the ρ parameter on the Zee-model in the limit of $\chi\to 0$ is similar to effects of that on the THDM. Let us examine at the one-loop effect of the weak-singlet charged Higgs boson on the decay width of $h\to\gamma\gamma$ in the decoupling limit. Let us recall that in Fig. 8, the size of the new couplings σ_1 and

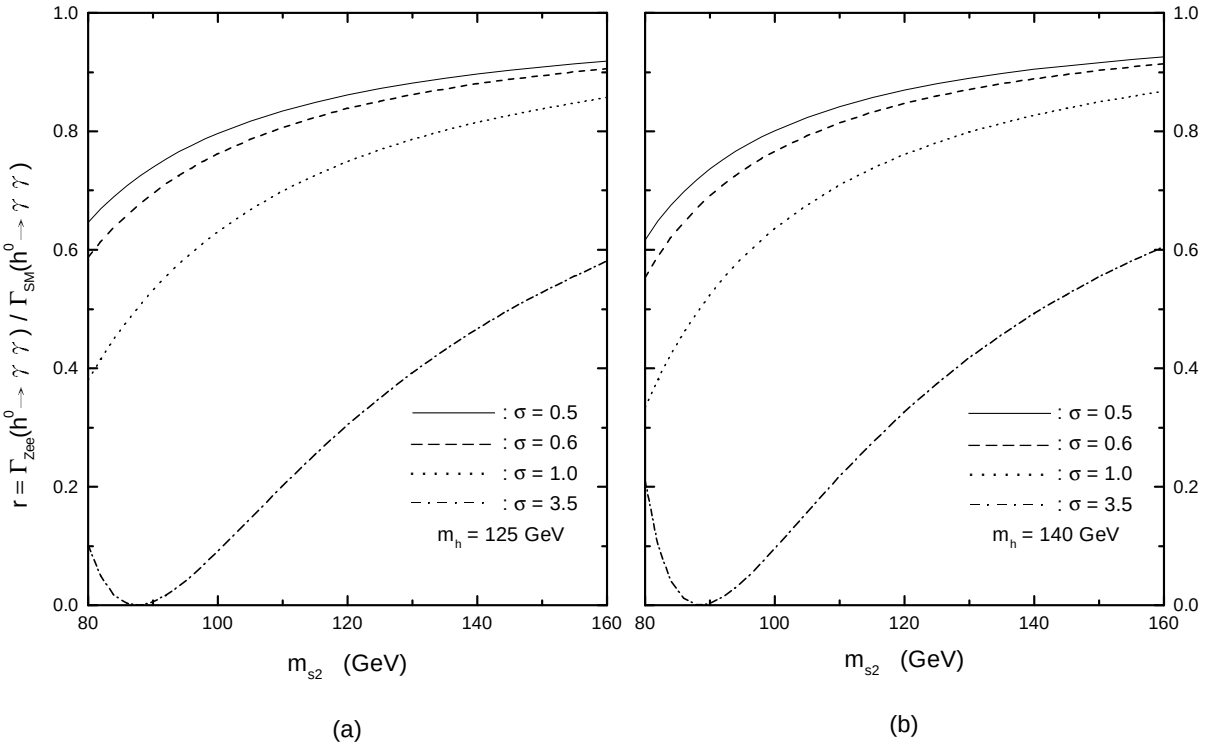

FIG. 10. (a) The ratio r as a function of the charged Higgs boson mass m_{S_2} for various values of the coupling constants $\sigma_1 = \sigma_2 \equiv \sigma$ with $m_h = 125$ GeV. The two smaller σ's are consistent with the cut-off scales $\Lambda = 10^{19}$ GeV and $\Lambda = 10^{16}$ GeV, respectively. The two larger σ's are allowed for $\Lambda = 10^4$ GeV. (b) A similar plot with $m_h = 140$ GeV.

σ_2 can be as large as 2 simultaneously, if the cut-off scale is at the order of 10^7 GeV. For the Zee-model to be a valid low energy effective theory up to 10^{19} GeV, σ_1 and σ_2 cannot be much larger than 0.6. To illustrate the implications of this result, we show in Figs. 10 (a) and 10 (b) the ratio (r) of the $h \to \gamma\gamma$ width predicted in the Zee-model to that in the SM, $r \equiv \Gamma_{\rm Zee}(h \to \gamma\gamma)/\Gamma_{\rm SM}(h \to \gamma\gamma)$, as a function of the coupling constant σ_2 and the charged Higgs boson mass m_{S_2}. Here, for simplicity, we have set $\sigma_1 = \sigma_2$ so that the $\tan\beta$ dependence drops in the decoupling case, cf. Eq. (42). For illustrations, we consider two cases for the mass of the lighter CP-even Higgs boson: $m_h = 125$ GeV and $m_h = 140$ GeV. As shown in the figures, the ratio r can be around 0.8 for $\sigma_1 = \sigma_2 \equiv \sigma \approx 0.5$ and $m_{S_2} \approx 100$ GeV. This reduction is due to the cancellation between the contribution from the S_2-boson

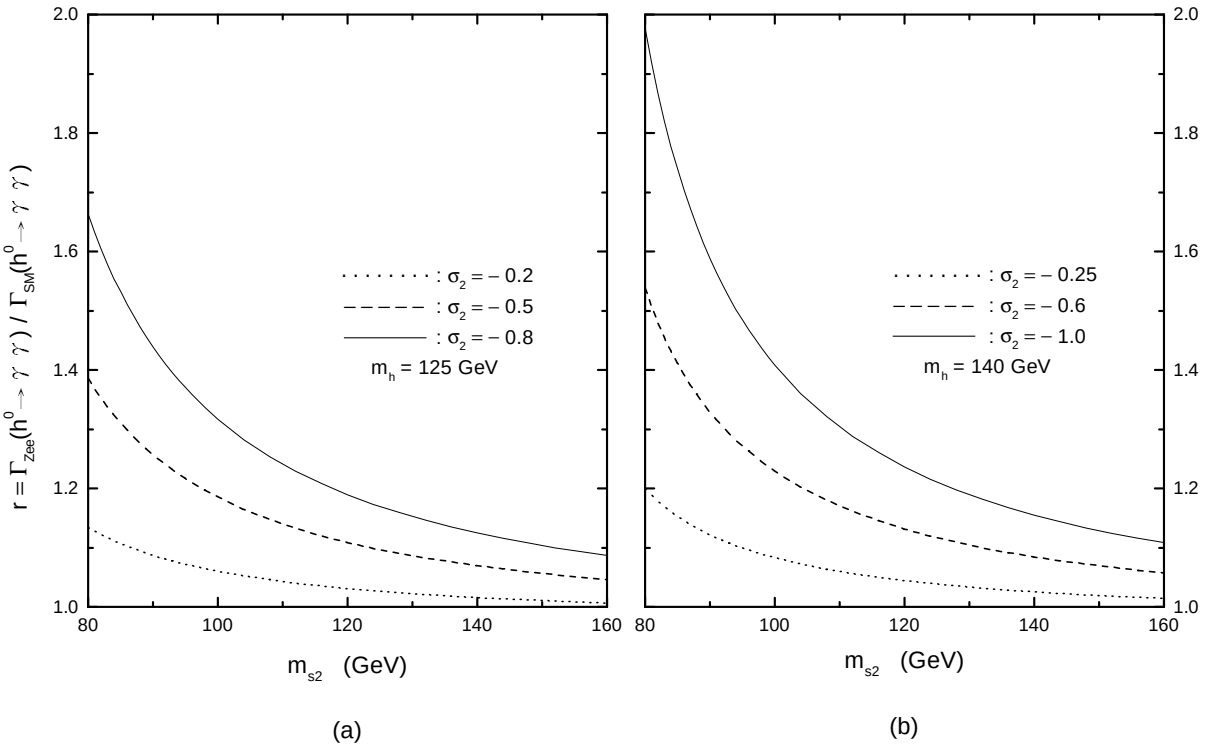

FIG. 11. (a) The ratio r as a function of the charged Higgs boson mass m_{S_2} for negative values of the coupling constants σ_2 with $m_h = 125$ GeV, $\sigma_1 = 0$ and $\tan\beta = 16\sqrt{2}$. The value $\sigma_2 = -0.2$, -0.5 or -0.8 is consistent with the cut-off scale $\Lambda = 10^{19}$, 10^7 or 10^4 GeV, respectively. (b) A similar plot with $m_h = 140$ GeV, $\sigma_1 = 0$ and $\tan\beta = 16\sqrt{2}$. The value $\sigma_2 = -0.25$, -0.6 or -1 is consistent with the cut-off scale $\Lambda = 10^{19}$, 10^7 or 10^4 GeV, respectively.

loop and the W-boson loop contributions. To have a similar reduction rate in $\Gamma_{\rm Zee}(h \to \gamma\gamma)$ for a heavier S_2, the coupling constant σ_2 (and σ_1) has to be larger. Next, as shown in Figs. 7 and 8, σ_1 and σ_2 do not have to take the same values in general, and they can be less than zero. In the case where both σ_1 and σ_2 are negative, the contribution of the S_2-loop diagram and that of the W-loop diagram have the same sign, so that r can be larger than 1. Such an example is shown in Fig. 11 (a), where the ratio r for $m_h = 125$ GeV is shown as a function of m_{S_2} at various negative σ_2 values with $\sigma_1 = 0$ and $\tan\beta = 16\sqrt{2}$. We consider the case with $\sigma_2 = -0.2$, -0.5 or -0.8, which is consistent with the cut-off scale $\Lambda = 10^{19}$, 10^7 or 10^4 GeV, respectively. In the case of $\Lambda = 10^{19}$ GeV (10^4 GeV), the deviation from the

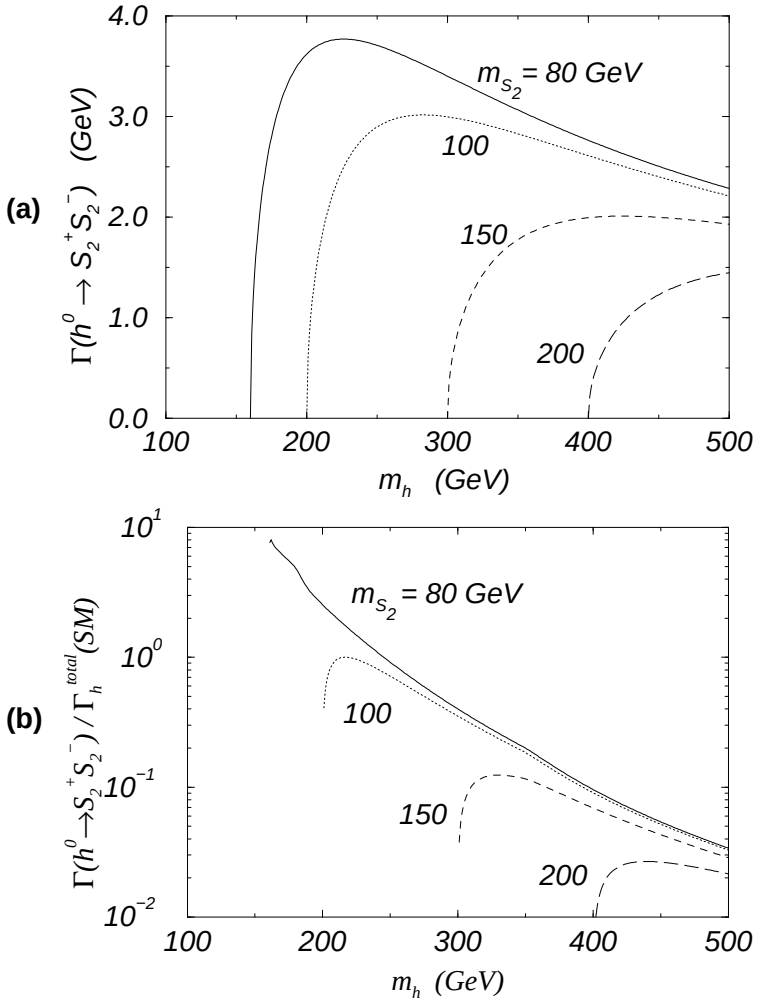

FIG. 12. (a) The partial decay width $\Gamma(h \to S_2^+ S_2^-)$ for $m_{S_2} = 80, 100, 150, 200$ GeV with $\sigma_1 = \sigma_2 = 1$ for the allowed range of m_h from 100 GeV to 500 GeV. (b) The ratio of $\Gamma(h \to S_2^+ S_2^-)$ with the total decay width of the SM Higgs boson for each values of m_{S_2}.

SM prediction can be about +6% (+30%) for $m_{S_2} = 100$ GeV. In Fig. 11 (b), the similar plot of the ratio r is shown for $m_h = 140$ GeV with $\sigma_1 = 0$ and $\tan\beta = 16\sqrt{2}$. Each case with $\sigma_2 = -0.25$, -0.6 or -1 is consistent with $\Lambda = 10^{19}$, 10^7 or 10^4 GeV, respectively. The correction is larger in the case with $m_h = 140$ GeV than in the case with $m_h = 125$ GeV for a given Λ. The deviation from the SM prediction can amount to about +8% (+40%) for $\Lambda = 10^{19}$ GeV (10^4 GeV) when $m_{S_2} = 100$ GeV. Larger positive corrections are obtained for smaller m_{S_2} values. Such a deviation from the SM prediction can be tested at the LHC, the e^+e^- LC and the $\gamma\gamma$ option of LC.

Before concluding this section, we remark that if m_h is larger than $2m_{S_2}$ such that the decay mode $h \to S_2^+ S_2^-$ is open, the total decay width of h can be largely modified from the SM prediction for large $\sigma_{1,2}$. In terms of R_{S_2}, the partial decay width of $h \to S_2^+ S_2^-$ is given by

$$\Gamma(h \to S_2^+ S_2^-) = \frac{c^2 v^2}{16\pi m_h} \sqrt{1 - \frac{4m_{S_2}^2}{m_h^2}}\,, \tag{43}$$

where $c^2 = (2m_{S_2}^2 R_{S_2}/v^2)^2$. In Fig. 12 (a), we show the partial decay width $\Gamma(h \to S_2^+ S_2^-)$ for $m_{S_2} = 80, 100, 150, 200$ GeV with $\sigma_1 = \sigma_2 = 1$, cf. Eq. (42), for the allowed range of m_h from 100 GeV to 500 GeV. In Fig. 12 (b), the ratio of $\Gamma(h \to S_2^+ S_2^-)$ to the total width of the SM Higgs boson ($\Gamma_h^{\rm total}(SM)$) is shown as a function of m_h for each value of m_{S_2}. This is to illustrate the possible size of the difference between the total width of the lightest CP-even Higgs boson h in the Zee-model and that of the SM Higgs boson[11]. Clearly, the impact of the $S_2^+ S_2^-$ decay channel is especially large in the small m_h region. We note that $\Gamma_h^{\rm total}(SM)$ can be determined to the accuracy of 10-20% at the LHC and the LC if $m_h < 2m_Z$, and to that of a couple of per cents if $m_h > 2m_Z$ [23]. (m_Z is the mass of the Z-boson.) Hence, measuring the total width of the lightest neutral Higgs boson can provide a further test of the Zee-model for $m_h > 2m_{S_2}$. The change in the total width also modifies the decay branching ratio of $h \to ZZ$, hence yields a different rate of $h \to ZZ \to \mu^+\mu^-\mu^+\mu^-$ for a given m_h. (In the SM, the branching ratio of $h \to ZZ$ is about 1/3 for $m_h > 200$ GeV.) Needless to say that for $m_h > 2m_{S_2}$, the production mode of $h \to S_2^+ S_2^- \to \ell^+\ell'^- \not{E}_T$ is also useful to test the Zee-model. Further discussion on this possibility will be given in Sec. VI.

---

[11] In doing this analysis, we have in mind a low cut-off scale $\Lambda = 10^4$ GeV, which allows a wide range of values for σ's, m_{S_2} and m_h.

V. PHENOMENOLOGY OF CHARGED-HIGGS BOSONS

In the Zee-model, two kinds of charged Higgs bosons appear. If there is no mixing between them ($\chi = 0$), the mass eigenstates $S_1^\pm$ and $S_2^\pm$ correspond to the THDM-like charged Higgs field and the singlet Higgs field $\omega^\pm$, respectively. The case with $\chi = 0$ occurs in the limit of $M^2 \gg v^2, \mu^2$ and m_0^2; i.e. in the decoupling limit. The detection of $S_2^\pm$ can be a clear indication of the Zee-model. As to be shown later, its phenomenology is found to be drastically different from that of the THDM-like charged Higgs bosons $S_1^\pm$ [24]. Here, we discuss how the effects of this extra charged boson can be explored experimentally. We first consider the case with $\chi = 0$, and then extend the discussion to the case with a non-zero χ.

The S_2^- boson decays into a lepton pair $e_i^- \overline{\nu}_{e_j}^c$ with the coupling constant f_{ij}. The partial decay rate, $\Gamma_{ij}^{S_2} = \Gamma(S_2^- \to e_i^- \overline{\nu}_{e_j}^c)$, is calculated as

$$\Gamma_{ij}^{S_2} = \frac{m_{S_2}}{4\pi} {f_{ij}}^2 \left(1 - \frac{m_{e_i}^2}{m_{S_2}^2}\right)^2, \tag{44}$$

and the total decay width of S_2^- is given by

$$\Gamma_{\rm total}^{S_2} = \sum_{i,j=1}^{3} \Gamma_{ij}^{S_2}. \tag{45}$$

By taking into account the hierarchy pattern of f_{ij}, cf. Eqs. (23) and (24), and by assuming $m_{S_2} = 100$ GeV and $|f_{12}| = 3 \times 10^{-4}$, the total decay width and the life time (τ) is estimated to be[12]

$$\Gamma_{\rm total}^{S_2} \sim \Gamma_{12}^{S_2} + \Gamma_{21}^{S_2} \sim 1.6 \text{ keV}, \tag{46}$$

$$\tau \sim 1/\Gamma_{\rm total}^{S_2} \sim 10^{-18} \text{sec}. \tag{47}$$

This implies that S_2 decays after traveling a distance of $\sim 10^{-10}$ m, which is significantly

[12]The size of the decay width depends on the value of f_{12}. If we take $m_{S_1} > 500$ GeV or $\mu < 100$ GeV, f_{12} can become one order of magnitude larger than 3×10^{-4}, while still being consistent with the phenomenological bounds discussed in Sec. II.

shorter than the typical detector scale. Therefore, $S_2^\pm$ decays promptly after its production, and can be detected at collider experiments.

The main production channel at the LEP-II experiment may be the pair production process $e^+e^- \to S_2^+S_2^-$, similar to the production of the THDM-like charged Higgs boson S_1^+. The matrix-element squares for the $S_i^+S_i^-$ production ($i = 1, 2$) are given by

$$\left|\mathcal{M}(e^-_{L(R)}e^+_{R(L)} \to S_i^+S_i^-)\right|^2 = \left\{\frac{Q_e e^2}{s} - \frac{1}{c_W^2}(I^3_{S_i} - s_W^2 Q_{S_i})\frac{(I_e^3 - s_W^2 Q_e)g^2}{s - m_Z^2}\right\}^2 s^2\beta^2_{S_i}\sin^2\Theta, \quad (48)$$

where $Q_e = -1$ and $I_e^3 = -\frac{1}{2}$ (0) for the incoming electron e_L^- (e_R^-); $Q_{S_i} = -1$ and $I^3_{S_i} = -\frac{1}{2}$ (0) for $i = 1$ (2); $\beta_{S_i} = \sqrt{1 - 4m^2_{S_i}/s}$, $s_W = \sin\theta_W$, $c_W = \cos\theta_W$, and Θ is the scattering angle of S_i^- in the e^+e^- center-of-mass (CM) frame whose energy is $\sqrt{s}$. For the other electron-positron helicity configuration ($e_L^-e_L^+$ and $e_R^-e_R^+$), the cross sections are zero. Thus the total cross section for the $S_2^+S_2^-$ pair production is given by

$$\sigma(e^+e^- \to S_2^+S_2^-) = \frac{1}{96\pi}\, e^4\beta^3_{S_2} s\left[\left(\frac{1}{s} + \frac{s_W^2}{c_W^2}\frac{1}{s - m_Z^2}\right)^2 + \left\{\frac{1}{s} - \left(\frac{1}{2} - s_W^2\right)\frac{1}{c_W^2}\frac{1}{s - m_Z^2}\right\}^2\right]. \quad (49)$$

Hence, the production rates of S_1^- and S_2^- are different. We note that the ratio of cross sections for $S_1^+S_1^-$ and $S_2^+S_2^-$ production, $\sigma(e^+e^- \to S_2^+S_2^-)/\sigma(e^+e^- \to S_1^+S_1^-)$, is 0.8 at $\sqrt{s} = 210$ GeV assuming that the masses of $S_1^\pm$ and $S_2^\pm$ are the same. This ratio is independent of the masses of S_1 and S_2 for a fixed CM energy. (Only the difference between $S_1^+S_1^-Z$ and $S_2^+S_2^-Z$ coupling constants determines this ratio.)

The lower mass bound of the THDM-like charged boson $S_1^\pm$ can be obtained by studying its $\tau\nu$ and cs decay modes, completely in the same way as the charged Higgs boson search in the minimal supersymmetric standard model (MSSM) [22]. Similar experimental constraints may be obtained for the extra charged bosons $S_2^\pm$. The situation, however, turns out to be fairly different from the $S_1^\pm$ case. First of all, decays of $S_2^\pm$ are all leptonic. Secondly, the branching ratios of various $S_2^\pm$ decay modes are estimated as

$$B(S_2^- \to e^-\not{E}_T) \sim 0.5, \quad (50)$$

$$B(S_2^- \to \mu^-\not{E}_T) \sim 0.5, \quad (51)$$

$$B(S_2^- \to \tau^-\not{E}_T) \sim \mathcal{O}\left(\frac{m_\mu^4}{m_\tau^4}\right) \sim 10^{-5}, \quad (52)$$

where we have used the relations given in Eqs. (23) and (24). Clearly, the branching ratio into the $\tau^- \not{E}_T$ mode is very small, so that it is not useful for detecting $S_2^\pm$ at all. This is different from the case of detecting the ordinary THDM-like charged Higgs boson, which preferentially decays into heavy fermion pairs (e.g. $\tau\nu$ and cs). Instead of studying the $\tau^\pm \nu^c$ mode, the $e^\pm \nu^c$ and $\mu^\pm \nu^c$ modes can provide a strong constraint on the mass of $S_2^\pm$. In fact, the branching ratio of $S_2^- \to e^- \not{E}_T$ or $\mu^- \not{E}_T$ is almost 100 %, so that we have $\sigma(e^+e^- \to S_2^+ S_2^- \to \ell^+\ell'^- \not{E}_T) \sim \sigma(e^+e^- \to S_2^+ S_2^-)$, where ℓ^- and ℓ'^- represent e^- or μ^- (not τ^-). Let us compare this with the cross section $\sigma(e^+e^- \to W^+W^- \to \ell^+\ell'^- \not{E}_T) = \sigma(e^+e^- \to W^+W^-)\cdot B(W^- \to \ell^- \not{E}_T)^2$, where $B(W^- \to \ell^- \not{E}_T) = B(W^- \to e^- \not{E}_T) + B(W^- \to \mu^- \not{E}_T) \sim 21\%$. As seen in Fig. 13, the cross section $\sigma(e^+e^- \to S_2^+ S_2^- \to \ell^+\ell'^- \not{E}_T)$ is comparable with $\sigma(e^+e^- \to W^+W^- \to \ell^+\ell'^- \not{E}_T)$. Therefore, by examining the LEP-II data for $\ell^+\ell'^- \not{E}_T$ (where $\ell^+\ell'^- = e^+e^-$, $e^\pm\mu^\mp$ or $\mu^+\mu^-$, in contrast to $\tau^+\tau^-$ for the $S_1^\pm$ case), the experimental lower bound on the mass of $S_2^\pm$ can be determined. Such a bound can be induced from the smuon search results at the LEP experiments [25,26] in the case that neutralinos are assumed to be massless. From the $\mu^+\mu^- \not{E}_T$ data accumulated up to $\sqrt{s} = 202$ GeV [26], we find that the lower mass bound of $S_2^\pm$ is likely to be 80-85 GeV for the $\chi = 0$ cases. [We note that the right-handed smuon ($\tilde{\mu}_R^\pm$) in the MSSM carries the same $SU(2) \times U(1)$ quantum number as the weak-singlet charged Higgs boson ($S_2^\pm$ for $\chi^\pm \sim 0$).]

We next comment on $S_2^\pm$-production processes at hadron colliders and future LC's. At hadron colliders, the dominant production mode is the pair production through the Drell-Yan-type process. The cross sections for $p\overline{p} \to S_2^+ S_2^-$ at the Tevatron Run-II energy ($\sqrt{s} = 2$ TeV) and $pp \to S_2^+ S_2^-$ at the LHC energy ($\sqrt{s} = 14$ TeV) are shown as a function of m_{S_2} in Fig. 14 for $\chi = 0$. At future LC's, the $S_2^\pm$ boson may be discovered through the above-discussed pair-production process from the electron-positron annihilation if $\sqrt{s}/2 > m_{S_2}$. In Fig. 15, we show the total cross section of $e^+e^- \to S_2^+ S_2^-$ for $\chi = 0$ as a function of m_{S_2} for $\sqrt{s} = 300$, 500, and 1000 GeV.

Finally, we like to discuss the case with a non-zero χ, in which S_2^- is a mixture of the singlet charged Higgs boson state (ω^-) and the doublet charged Higgs boson state (H^-). Let

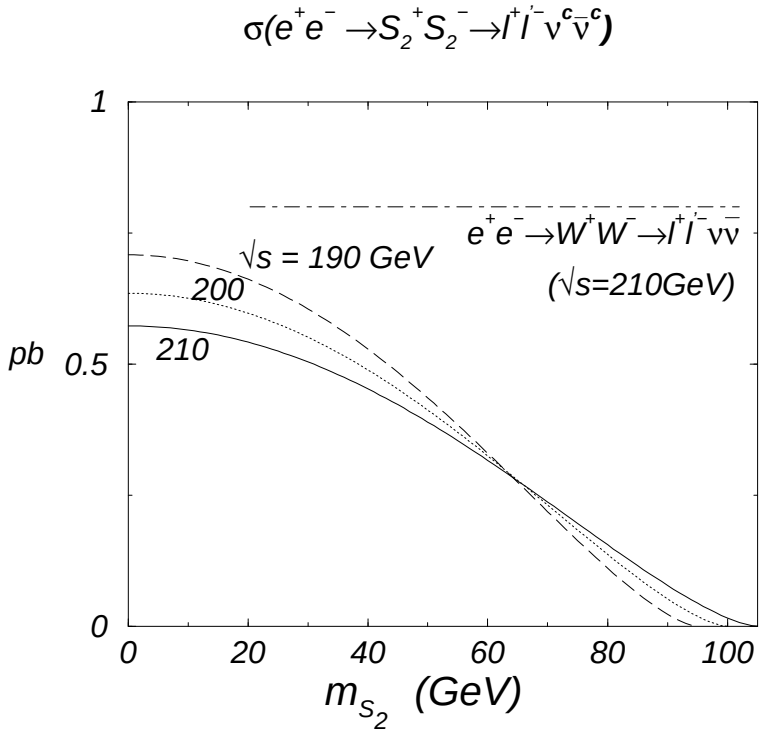

FIG. 13. The cross section of the leptonic decay process $e^+e^- \to S_2^+ S_2^- \to \ell^+\ell'^- \not{E}_T$ (where ℓ and $\ell' = e$ or μ) at $\sqrt{s} = 190$, 200, 210 GeV. The process $e^+e^- \to W^+W^- \to \ell^+\ell'^- \not{E}_T$ at $\sqrt{s} = 210$GeV is shown for comparison.

us see how the above discussion is changed in this case. The doublet charged Higgs bosons with the mass of 100 GeV mainly decay into the $\tau^-\nu$ and $\overline{c}s$ channels. Thus, the branching ratio of the decay process $S_2^- \to \ell^- \not{E}_T$, where ℓ^- represents e^- and μ^-, is expressed in a non-zero χ case as

$$B(S_2^- \to \ell^- \not{E}_T) = \frac{\cos^2\chi\ \Gamma^{S_2}_{\rm total}|_{\chi=0}}{\sin^2\chi\ \Gamma^{S_1}_{\rm total}|_{\chi=0} + \cos^2\chi\ \Gamma^{S_2}_{\rm total}|_{\chi=0}}, \tag{53}$$

where $\Gamma^{S_i}_{\rm total}|_{\chi=0}$ $(i = 1, 2)$ is the total width of S_i^- at $\chi = 0$ with the same mass as the decaying S_2^- on the left-hand side of the above equation. The formula of $\Gamma^{S_2}_{\rm total}|_{\chi=0}$ is given in Eq. (45), while $\Gamma^{S_1}_{\rm total}|_{\chi=0}$, which is the same as the total decay width of the charged Higgs boson in the THDM is given by

$$\Gamma^{S_1}_{\rm total}|_{\chi=0} = \sum_{\overline{f}f'} \Gamma(S_1^- \to \overline{f}f'), \tag{54}$$

where $\overline{f}f'$ are fermion pairs which are kinematically allowed. In the type-II Yukawa couplings, we have

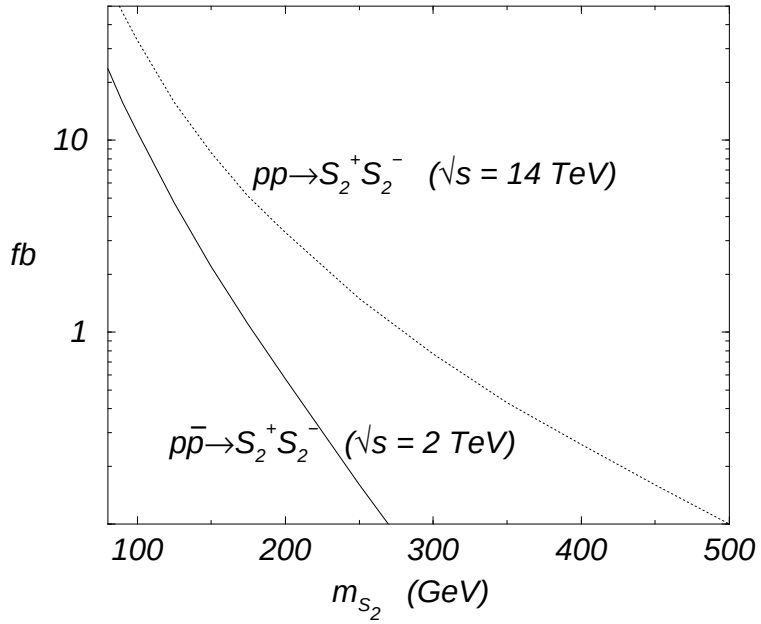

FIG. 14. The total cross sections of $p\overline{p} \to S_2^+ S_2^-$ at $\sqrt{s} = 2$ TeV (solid curve) and $pp \to S_2^+ S_2^-$ at $\sqrt{s} = 14$ TeV (dotted curve) as a function of m_{S_2}.

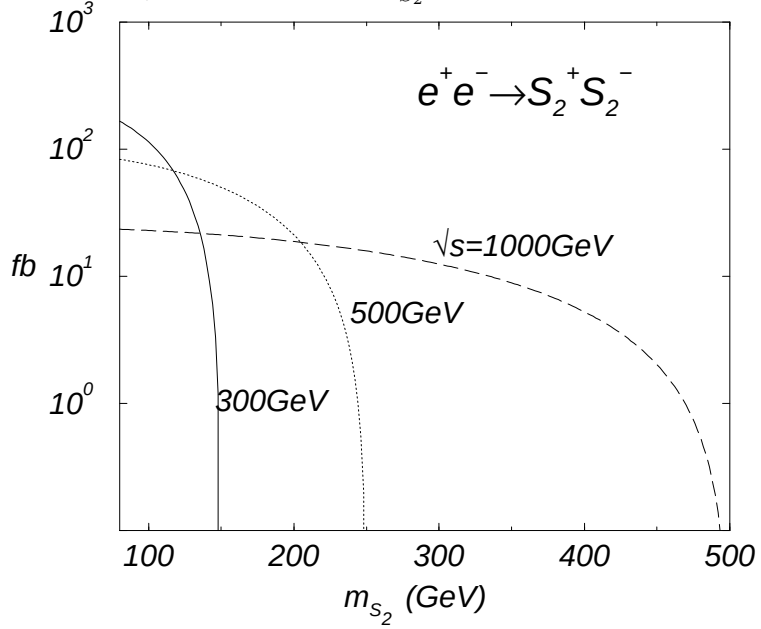

FIG. 15. The total cross section of $e^+e^- \to S_2^+ S_2^-$ as a function of m_{S_2} at $\sqrt{s} = 300$, 500 and 1000 GeV.

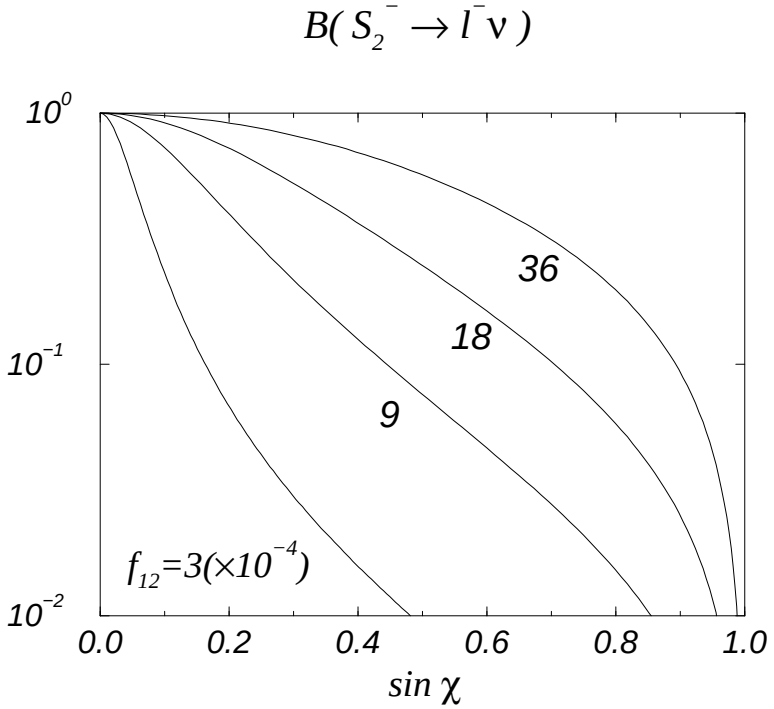

FIG. 16. The decay branching ratio of $S_2^- \to \ell^- \not{E}_T$ (where $\ell^- = e^-$ or μ^-) as a function of the mixing angle χ for $m_{S_2} = 100$ GeV, $\tan\beta = 1$ and various values of the coupling constant f_{12}.

$$\Gamma(S_1^- \to \tau^- \nu) = \frac{m_{S_1}}{8\pi v^2}(m_\tau^2 \tan^2\beta)\left(1 - \frac{m_\tau^2}{m_{S_1}^2}\right)^2, \tag{55}$$

$$\Gamma(S_1^- \to \overline{c}s) \simeq \frac{3m_{S_1}}{8\pi v^2}(m_s^2 \tan^2\beta + m_c^2 \cot^2\beta)\left(1 - \frac{m_c^2}{m_{S_1}^2}\right)^2, \tag{56}$$

$$\Gamma(S_1^- \to \overline{t}b) \simeq \frac{3m_{S_1}}{8\pi v^2}(m_b^2 \tan^2\beta + m_t^2 \cot^2\beta)\left(1 - \frac{m_t^2}{m_{S_1}^2}\right)^2. \tag{57}$$

In the THDM, the total decay width of the charged Higgs boson (H^-) for $m_{H^-} = 100$ GeV is about 470 keV. Hence, if the mixing angle χ is not so small, the decay pattern of S_2^- is dominated by that of the THDM charged Higgs boson H^-. In Fig. 16, we plot the branching ratio $B(S_2^- \to \ell^- \not{E}_T)$ as a function of $\sin\chi$ at $m_{S_2} = 100$ GeV for several values of f_{12}. We only show the case with $\tan\beta = 1$, where the result is independent of the type of the Yukawa interaction. The coupling constant f_{12} is taken to be $3, 9, 18$ and 36 ($\times 10^{-4}$), which satisfy the phenomenological constraints given in Sec. II. As expected, the branching ratio decreases as χ increases. When $f_{12} = 36 \times 10^{-4}$, $B(S_2^- \to \ell^- \not{E}_T)$ is smaller than 10% for $\sin\chi > 0.89$.

For the smaller f_{12} values, the branching ratio reduces more quickly. The branching ratio is not sensitive to m_{S_2} unless the mass exceeds the threshold of the decay into a $\overline{t}b$ or h^0W^- pair. Above the threshold of the $\overline{t}b$ pair production, the decay rate of $S_2^- \to \overline{t}b$ is large due to the large mass of the top quarks, so that $B(S_2^- \to \ell^- \not{E}_T)$ is substantial only for very small values of χ. Finally, while the decay branching ratio can change drastically depending on the mixing angle χ, the production cross section for $e^+e^- \to S_2^+ S_2^-$ remains unchanged. In conclusion, the process $e^+e^- \to S_2^+ S_2^- \to \ell^+\ell'^- \not{E}_T$ can also be useful for testing the Zee-model in the non-zero χ case, provided $\sin\chi$ is not too large.

VI. DISCUSSION AND CONCLUSION

In this paper, the Higgs sector of the Zee-model has been investigated, in which neutrino masses are generated radiatively. This model contains extra weak-doublet Higgs field and singlet charged Higgs field.

We have studied indirect effects of these extra Higgs bosons on the theoretical mass bounds of the lightest CP-even Higgs boson, which are obtained from the requirement that the running coupling constants neither blow up to a very large value nor fall down to a negative value, up to a high-energy cut-off scale Λ. For $\Lambda = 10^{19}$ GeV, the upper bound of m_h is found to be about 175 GeV, which is almost the same value as the SM prediction. In the decoupling regime ($M \gg m_Z$), the lower bound is found to be about 100 GeV for $\Lambda = 10^{19}$ GeV, which is much smaller than the lower bound in the SM, and is almost the same as that in the THDM. For smaller Λ values, the bounds are more relaxed, similar to that of the SM. We have also investigated the allowed range of the coupling constants relevant to the weak-singlet Higgs field.

The most striking feature of the Zee-model Higgs sector is the existence of the weak-singlet charged Higgs boson. We have examined the possible impact of the singlet charged-Higgs boson on the neutral Higgs boson search through radiative corrections. We found that its one-loop contributions to the $h \to \gamma\gamma$ width can be sizable. In the allowed range

of the coupling constants the deviation from the SM prediction for this decay width can be about -20% or near $+10\%$ for $m_{S_2} = 100$ GeV and $\Lambda = 10^{19}$ GeV, depending on the sign of the coupling constants σ_i. The magnitude of the deviation is larger for lower Λ values or for smaller m_{S_2} values. For example, a positive deviation over 30-40% is possible for $m_h = 125$-140 GeV, $m_{S_2} = 100$ GeV, and $\Lambda = 10^4$ GeV.

In the decoupling limit (i.e. when $M^2 \gg v^2$, where $\alpha \to \beta - \pi/2$ and $\chi \to 0$), we expect that the production cross sections for $gg \to h$, $e^+e^- \to \nu\overline{\nu}h$ and $e^+e^- \to Z^0h$ in the Zee-model are the same as those in the SM. However, a sizable change in the decay branching ratio of $h \to \gamma\gamma$ can alter the production rate of $pp \to hX \to \gamma\gamma X$ at the LHC, where this production rate can be determined with a relative error of 10-15% [15]. Also, such a deviation in the branching ratio of $h \to \gamma\gamma$ directly affects the cross section of $e^+e^- \to \nu\overline{\nu}h$ (andZ^0h) $\to \nu\overline{\nu}\gamma\gamma$, which can be measured with an accuracy of 16-22% at the future e^+e^- LC (with $\sqrt{s} = 500$ GeV and the integrated luminosity of 1 ab^{-1}) [16]. Therefore, the Zee-model with low cut-off scales can be tested through the $h \to \gamma\gamma$ process at the LHC and the e^+e^- LC's. At the future photon colliders, the enhancement (or reduction) of the $h \to \gamma\gamma$ partial decay rate will manifest itself in the different production rate of h from the SM prediction. A few per cent of the deviation in $\Gamma(h \to \gamma\gamma) \cdot B(h \to b\overline{b})$ can be detected at a photon collider [17], so that the effects of the singlet charged Higgs boson can be tested even if the cutoff scale Λ is at the Planck scale.

The collider phenomenology of the singlet charged Higgs boson has turned out to be completely different from that of the THDM-like charged Higgs boson. The singlet charged Higgs boson mainly decays into $\ell^\pm \not{E}_T$ (with $\ell^\pm = e^\pm$ or $\mu^\pm$), while the decay mode $\tau^\pm \not{E}_T$ is almost negligible due to the relation $|f_{12}| \gg |f_{13}| \gg |f_{23}|$. This hierarchy among the coupling constants f_{ij} results from demanding bi-maximal mixings in the neutrino mass matrix generated in the Zee-model to be consistent with the neutrino oscillation data. On the other hand, the THDM-like charged Higgs boson decays mainly into either the $\tau\nu$ mode or the cs mode, through the usual Yukawa-interactions. Hence, to probe this singlet charged Higgs boson using the LEP-II data, experimentalists should examine their data sample with

$e^+e^-\not{E}_T$, $e^+\mu^-\not{E}_T$, $\mu^+e^-\not{E}_T$ or $\mu^+\mu^-\not{E}_T$, while the experimental lower mass bound of the THDM-like charged Higgs boson is obtained from examining the $\tau\tau\not{E}_T$, $\tau\not{E}_T\, jj$ and $jjjj$ events. Using the published LEP-II constraints on the MSSM smuon production (assuming the lightest neutralinos to be massless), we estimate the current lower mass bound of this singlet charged Higgs boson to be about 80-85 GeV. The Tevatron Run-II, LHC and future LC's can further test this model.

Finally, we comment on a case in which the singlet charged Higgs boson ($S_2^\pm$ for $\chi = 0$) is the lightest of all the Higgs bosons. For $m_h/2 > m_{S_2} > m_Z$, the Higgs sector of the Zee-model can be further tested by measuring the production rate of pp (or $p\overline{p}$) $\to hX \to S_2^+ S_2^- X \to \ell^+\ell'^-\not{E}_T\, X$. The branching ratio for $h \to S_2^+ S_2^- \to \ell^+\ell'^-\not{E}_T$ can be large. For instance, for $m_h = 210$ GeV and $m_{S_2} = 100$ GeV, this branching ratio is about 12% for each $\ell^+\ell'^- = e^+e^-$, $e^+\mu^-$, μ^+e^- or $\mu^+\mu^-$. The branching ratio decreases for larger masses of h. Moreover, the total decay width of h can be largely modified when the decay channel $h \to S_2^+ S_2^-$ is open. In this case, the decay branching ratios of $h \to W^+W^-$, ZZ are also different from the SM predictions.

In conclusion, the distinguishable features of the Zee-model from the SM and the THDM can be tested by the data from LEP-II, the Tevatron Run-II and future experiments at LHC and LC's.

ACKNOWLEDGMENTS

We are grateful to the warm hospitality of the Center for Theoretical Sciences in Taiwan where part of this work was completed. CPY would like to thank H.-J. He, J. Ng and W. Repko for stimulating discussions. SK was supported, in part, by the Alexander von Humboldt Foundation. GLL and JJT were supported, in part, by the National Science Council of R.O.C. under the Grant No NSC-89-2112-M-009-035; YO was supported by the Grant-in-Aid of the Ministry of Education, Science, Sports and Culture, Government of Japan (No. 09640381), Priority area "Supersymmetry and Unified Theory of Elementary

Particles" (No. 707), and "Physics of CP Violation" (No. 09246105); CPY is supported by the National Science Foundation in the USA under the grant PHY-9802564.

APPENDIX: ONE-LOOP RGE'S FOR DIMENSIONLESS COUPLING CONSTANTS

Here, we summarize the relevant RGE's to our study. For the gauge coupling constants, we have

$$\mu\frac{d}{d\mu}g_1 = \frac{1}{16\pi^2}\frac{22}{3}g_1^3, \tag{A1}$$

$$\mu\frac{d}{d\mu}g_2 = \frac{1}{16\pi^2}\left(-3\right)g_2^3, \tag{A2}$$

$$\mu\frac{d}{d\mu}g_3 = \frac{1}{16\pi^2}\left(-7\right)g_3^3. \tag{A3}$$

The RGE's for the Higgs-self-coupling constants of the doublets are calculated at the one-loop level as

$$\begin{aligned}\mu\frac{d}{d\mu}\lambda_1 = \frac{1}{16\pi^2}\Big\{&12\lambda_1^2 + 4\lambda_3^2 + 4\lambda_3\lambda_4 + 2\lambda_4^2 + 2\lambda_5^2 + 2\sigma_1^2 \\ &- \left(3g_1^2 + 9g_2^2\right)\lambda_1 + \left(\frac{3}{4}g_1^4 + \frac{3}{2}g_1^2g_2^2 + \frac{9}{4}g_2^4\right)\Big\},\end{aligned} \tag{A4}$$

$$\begin{aligned}\mu\frac{d}{d\mu}\lambda_2 = \frac{1}{16\pi^2}\Big\{&12\lambda_2^2 + 4\lambda_3^2 + 4\lambda_3\lambda_4 + 2\lambda_4^2 + 2\lambda_5^2 + 2\sigma_2^2 + 12y_t^2\lambda_2 - 12y_t^4 \\ &- \left(3g_1^2 + 9g_2^2\right)\lambda_2 + \left(\frac{3}{4}g_1^4 + \frac{3}{2}g_1^2g_2^2 + \frac{9}{4}g_2^4\right)\Big\},\end{aligned} \tag{A5}$$

$$\begin{aligned}\mu\frac{d}{d\mu}\lambda_3 = \frac{1}{16\pi^2}\Big\{&2\left(\lambda_1 + \lambda_2\right)\left(3\lambda_3 + \lambda_4\right) + 4\lambda_3^2 + 2\lambda_4^2 + 2\lambda_5^2 + 2\sigma_1\sigma_2 + 6y_t^2\lambda_3 \\ &- \left(3g_1^2 + 9g_2^2\right)\lambda_3 + \left(\frac{3}{4}g_1^4 - \frac{3}{2}g_1^2g_2^2 + \frac{9}{4}g_2^4\right)\Big\},\end{aligned} \tag{A6}$$

$$\begin{aligned}\mu\frac{d}{d\mu}\lambda_4 = \frac{1}{16\pi^2}\Big\{&2\left(\lambda_1 + \lambda_2\right)\lambda_4 + 4\left(2\lambda_3 + \lambda_4\right)\lambda_4 + 8\lambda_5^2 + 6y_t^2\lambda_4 \\ &- \left(3g_1^2 + 9g_2^2\right)\lambda_4 + 3g_1^2g_2^2\Big\},\end{aligned} \tag{A7}$$

$$\mu\frac{d}{d\mu}\lambda_5 = \frac{1}{16\pi^2}\left\{2\lambda_1 + 2\lambda_2 + 8\lambda_3 + 12\lambda_4 + 6y_t^2 - \left(3g_1^2 + 9g_2^2\right)\right\}\lambda_5, \tag{A8}$$

and those with respect to the additional singlet charged Higgs are given by

$$\begin{aligned}\mu\frac{d}{d\mu}\sigma_1 = \frac{1}{16\pi^2}\Big\{&4\sigma_1^2 + 2\sigma_1\sigma_3 + 6\lambda_1\sigma_1 + \left(4\lambda_3 + 2\lambda_4\right)\sigma_2 + 8f_{ij}f_{ij}\sigma_1 \\ &- \left(\frac{15}{2}g_1^2 + \frac{9}{2}g_2^2\right)\sigma_1 + 3g_1^4\Big\},\end{aligned} \tag{A9}$$

$$\mu\frac{d}{d\mu}\sigma_2 = \frac{1}{16\pi^2}\left\{4\sigma_2^2 + 2\sigma_2\sigma_3 + 6\lambda_2\sigma_2 + \left(4\lambda_3 + 2\lambda_4\right)\sigma_1 + 6y_t^2\sigma_2 + 8f_{ij}f_{ij}\sigma_2\right.$$

$$- \left(\frac{15}{2} g_1^2 + \frac{9}{2} g_2^2 \right) \sigma_2 + 3 g_1^4 \Big\} , \tag{A10}$$

$$\mu \frac{d}{d\mu} \sigma_3 = \frac{1}{16\pi^2} \left\{ 8\sigma_1^2 + 8\sigma_2^2 + 5\sigma_3^2 + 16 f_{ij} f_{ij} \sigma_3 - 128\, tr\, f^4 - 12 g_1^2 \sigma_3 + 24 g_1^4 \right\} . \tag{A11}$$

Finally, the RGE's for the Yukawa-type coupling constants are obtained at one-loop level as

$$\mu \frac{d}{d\mu} y_t = \frac{1}{16\pi^2} \left\{ - \left(\frac{17}{12} g_1^2 + \frac{9}{4} g_2^2 + 8 g_3^2 \right) y_t + \frac{9}{2} y_t^3 \right\} , \tag{A12}$$

$$\mu \frac{d}{d\mu} f_{ij} = \frac{1}{16\pi^2} \left\{ - \left(\frac{3}{2} g_1^2 + \frac{9}{2} g_2^2 \right) f_{ij} + 4 f_{kl} f_{kl} f_{ij} - 4 f_{ik} f_{kl} f_{lj} \right\} , \tag{A13}$$

where

$$tr\, f^4 \equiv \sum_{i,j,k,l=1-3} f_{ij} f_{jk} f_{kl} f_{li},$$

$$f_{ij} f_{ij} \equiv \sum_{i,j=1-3} f_{ij} f_{ij}.$$

REFERENCES

[1] Super-Kamiokande Collaboration, Y. Fukuda et al., *Phys. Rev. Lett.* **81** (1998) 1562.

[2] A. Zee, *Phys. Lett.* B **93** (1980) 339; *Phys. Lett.* B **161** (1985) 141.

[3] S.T. Petcov, *Phys. Rev.* D **115** (1982) 401; J. Liu, *Phys. Lett.* B **216** (1989) 367; B.K. Pal, *Phys. Rev.* D **44** (1991) 2261; W. Grimus, and G. Nardulli, *Phys. Lett.* B **271** (1991) 161; A.Y. Smirnov and Z.-J. Tao, *Nucl. Phys.* B **426** (1994) 415; P.H. Frampton and S.L. Glashow, *Phys. Lett.* B **461** (1999) 95; G.C. McLaughlin and J.N. Ng, *Phys. Lett.* B **464** (1999) 232; A.S. Jaurabh and S.D. Rindani, *Phys. Lett.* B **464** (1999) 239; K. Cheung, O.C.W. Kong, *Phys. Rev.* D **61** (2000) 113012; K. Cheung, O.C.W. Kong, `hep-ph/0003276`; Y. Koide and A. Ghosal, *Phys. Rev.* D **63** (2001) 037301.

[4] C. Jarlskog, M. Matsuda, S. Skadhauge, M. Tanimoto, *Phys. Lett.* B **449** (1999) 240.

[5] C. Jarlskog, M. Matsuda, S. Skadhauge, M. Tanimoto, (`hep-ph/0005147`).

[6] A.Yu. Smirnov, M. Tanimoto, *Phys. Rev.* D **55** (1997) 1665.

[7] G.C. McLaughlin and J.N. Ng, *Phys. Lett.* B **455** (1999) 224.

[8] ALEPH Collaboration, *Phys. Lett.* B **487** (2000) 253,

[9] "Report of the Higgs Working Group" from the Physics at Run II Supersymmetry/Higgs Workshop, `hep-ph/0010338`.

[10] CMS Technical Proposal, CERN/LHCC/94-38 (1994); ATLAS Technical Proposal, CERN/LHCC/94-93 (1994); ATLAS Technical Design Report, CERN/LHCC/99-15 (1999).

[11] N. Cabibbo, L. Maiani, G. Parisi and R. Petronzio, *Nucl. Phys.* B **158** (1976) 295; M. Lindner, *Z. Phys.* C **31** (1986) 295; G. Altarelli and I. Ishidori, *Phys. Lett.* B **337** (1994) 141; J.A. Casas, J.R. Espinosa, and M. Quirós, *Phys. Lett.* B **342** (1995) 171; *ibid.* B **382** (1996) 374; J.R. Espinosa and M. Quirós, *Phys. Lett.* B **353** (1995) 257; M. Quirós,

IEM-FT-153/97, in *Perspectives on Higgs Physics II, Ed. G.L. Kane*, World Scientific, Singapore; T. Hambye and K. Riesselmann, *Phys. Rev.* D **55** (1997) 7255.

[12] H. Komatsu, *Prog. Theor. Phys.* **67** (1982) 1177; R.A. Flores and M. Sher, *Ann. Phys. (NY)* **148** (1983) 295; M. Sher, *Phys. Rep.* **179** (1989) 273; D. Kominis and R.S. Chivukula, *Phys. Lett.* B **304** (1993) 152; S. Kanemura, T. Kubota and E. Takasugi, *Phys. Lett.* B **313** (1993) 155; S. Nie and M. Sher, *Phys. Lett.* B **449** (1999) 89; A. Akeroyd, A. Arhrib, E. Naimi, *Phys. Lett.* B **490** (2000) 119.

[13] S. Kanemura, T. Kasai, Y. Okada, *Phys. Lett.* B **471** (1999) 182.

[14] J. Casas, V. Clemente, A. Ibarra, M. Quirós, *Phys. Rev.* D **62** (2000) 053005.

[15] D. Zeppenfeld, R. Kinnunen, A. Nikitenko, and E. Richiter-Was, *Phys. Rev.* D **62** (2000) 013009.

[16] E. Boos, J.-C. Brient, D.W. Reid, H.J. Schreiber, and R. Schanidze, hep-ph/0011366; Rick van Kooten, Talk at the Berkeley Linear Collider Meeting in March 2000 (`http://needmore.physics.indiana.edu/~rickv/nlc/talks/Berkeley_2000/Berkeley_2000.html`).

[17] M. Melles, Talk given at LCWS 2000 (Fermilab, October 2000), `hep-ph/0012195`.

[18] Z. Maki, M. Nakagawa and S. Sakata, *Prog. Theor. Phys.* **28** (1962) 870.

[19] M. Ciuchini, G. Degrassi, P. Gambini and G.F. Giudice, *Nucl. Phys.* B **527** (1998) 21; P. Ciafaloni, A. Romanino and A. Strumia, *Nucl. Phys.* B **524** (1998) 361; F. Borzumati and G. Greub, *Phys. Rev.* D **58** (1998) 074004; T.M. Aliev and E.O. Iltan, *Phys. Rev.* D **58** (1998) 095014.

[20] H.E. Haber and H.E. Logan, *Phys. Rev.* D **62** (2000) 015011.

[21] J.F. Gunion, H.E. Haber, G. Kane and Sally Dawson, *The Higgs Hunters Guide*, Addison-Wesley Publishing Company (1990).

[22] ALEPH Collaboration, *Phys. Lett.* B **495** (2000) 1; L3 Collaboration, *Phys. Lett.* B **495** (2000) 18.

[23] V. Drollinger and A. Sopczak, `hep-ph/0102342`.

[24] S. Kanemura, T. Kasai, G.-L. Lin, Y. Okada, J.J. Tseng, and C.-P. Yuan, `hep-ph/0010233`.

[25] M. Dima, talk given at LCWS 2000 (Fermilab, October 2000) `http://www-lc.fnal.gov/lcws2000/`;
ALEPH Collaboration, *Phys. Lett.* B **407** (1997) 377.

[26] ALEPH Collaboration, *Phys. Lett.* B **487** (2000) 253.

(b)